Arnold Mathematical Journal
Volume 11, Issue 4, 2025

Spirals, tic-tac-toe partition, and deep diagonal maps

Zhengyu Zou

Received 25 Dec 2024; Accepted 9 Aug 2025

Abstract: The deep diagonal map T_k acts on planar polygons by connecting the k-th diagonals and intersecting them successively. The map T_2 is the pentagram map, and T_k is a generalization. We study the action of T_k on two subsets of the so-called twisted polygons, which we term *type-α and type-β k-spirals*. For $k \geq 2$, T_k preserves both types of k-spirals. In particular, we show that for $k = 2$ and $k = 3$, both types of k-spirals have precompact forward and backward T_k-orbits modulo projective transformations. We derive a rational formula for T_3, which generalizes the y-variables transformation formula of the corresponding quiver mutation by M. Glick and P. Pylyavskyy. We also present four algebraic invariants of T_3. These special orbits in the moduli space are partitioned into cells of a 3×3 tic-tac-toe grid. This establishes the action of T_k on k-spirals as a geometric generalization of T_2 on convex polygons.

DOI: 10.56994/ARMJ.011.004.006

AMS Classification: 05E99, 37J70, 51A05

Key words and phrases: pentagram map, twisted polygons, cluster algebra, polygonal dynamics, projective geometry, integrable systems, Casimir functions, discrete dynamical systems

1 Introduction

1.1 Context and Motivation

Given a polygon P in the real projective plane, let T_k be the map that connects its k-th diagonals and intersects them successively to form another polygon P' whose vertices are given by the following formula:

$$P'_i = P_iP_{i+k} \cap P_{i+1}P_{i+k+1}. \tag{1}$$

Figure 1 demonstrates an example of the action of T_2 on a convex heptagon. The map T_2 is called the *pentagram map*, a well-studied discrete dynamical system (see [Sch92, Sch01, Sch08, OST10]). A well-known result is that T_2 preserves convexity.[1] The T_2-orbit of a convex polygon sits on a flat torus in the moduli space of projective equivalent convex polygons. On the other hand, the geometry of the map T_k is less well-behaved. For $k \geq 3$, the T_k images of convex polygons may not even be embedded. See Figure 1 for an example of T_3 taking a convex heptagon to a polygon that is not even embedded.

Previous results of T_k often had an algebraic and combinatorial flavor, motivated by two branches of studies. The first one was a sequence of works [Sch08, OST10, Sol13, OST13] that established that the T_2 action on the moduli space of projective convex polygons is a discrete completely integrable system; the second one was M. Glick's discovery in [Gli11] of the connection between T_2 and cluster algebras. In [GSTV12], M. Gekhtman, M. Shapiro, S. Tabachnikov, and A. Vainshtein generalized the cluster transformations in [Gli11] to the map T_k acting on so-called "corrugated polygons," which

[1] A projective polygon is *convex* if some projective transformation maps it to a planar convex polygon in the affine patch

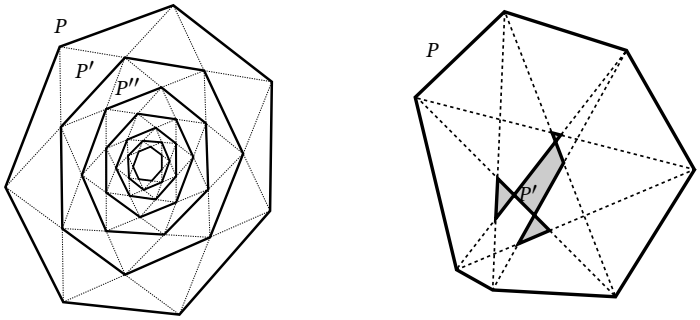

Figure 1: Left: The iterative images of a convex heptagon under the action of T_2. Right: A convex heptagon whose image under T_3 is not even embedded.

are polygonal curves in $\mathbb{RP}^k$ satisfying certain coplanarity conditions. [GSTV12] showed that T_k is a discrete integrable system. There are numerous integrability results for these higher-dimensional analogs. See [KS13, MB13, MB14, KS16, IK23]. These led to many applications and connections of T_k to other fields, such as octahedral recurrence [Sch08, FK12], the condensation method of computing determinants [Sch08, Gli18], cluster algebras [Gli11, GSTV12, GP16, FK12], Poisson Lie groups [FM16, Izo22b], T-systems [KV15, FK12], Grassmannians [FMB19], algebraically closed fields [Wei23], Poncelet polygons [Sch07, Sch21, Izo22a, Sch24], and integrable partial differential equations [Sch08, OST10, NS21].

The geometric aspects of T_k and other deep diagonal maps on planar polygons remain underexplored. There are only a few studies on the geometries of T_k that focused on small k or polygons with many symmetries. See [Sch21, Sch24]. There is no established general framework on the type of geometric properties preserved under T_k for $k \geq 3$ that is analogous to convexity under T_2. Even less is known for geometric objects that have precompact orbits under T_k.

The most relevant result to this endeavor is the discovery of *k-birds* under the map Δ_k in [Sch25]. A k-bird P is a planar n-gon with $n > 3k$, such that there exists a continuous

path of polygons $P^{(t)}$ connecting P to the regular n-gon where the four lines

$$P_i^{(t)}P_{i-k-1}^{(t)}, \quad P_i^{(t)}P_{i-k}^{(t)}, \quad P_i^{(t)}P_{i+k}^{(t)}, \quad P_i^{(t)}P_{i+k+1}^{(t)}$$

are distinct for all $i = 1, \dots, n$ and $t \in I$. The map Δ_k connects the $(k+1)$-th diagonal of a polygon and intersects the diagonals that are k clicks apart. See Figure 2 for the action of Δ_2 on 2-birds. In [Sch25], R. Schwartz showed that the k-birds are invariant under both Δ_k and Δ_k^{-1}. Experimentally, the k-birds seem to have toroidal orbits under Δ_k, which highly resembles the orbit of convex n-gons under T_2. Schwartz also showed that the k-birds have precompact forward Δ_k-orbits modulo affine transformations—a property satisfied by convex n-gons under T_2.

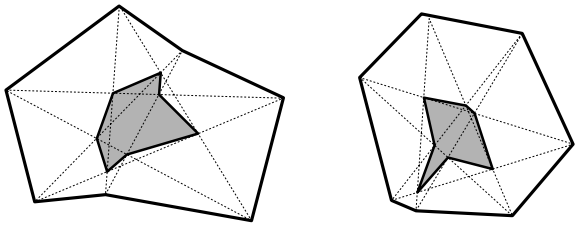

Figure 2: Action of Δ_2 on two heptagons that are 2-birds.

This paper has two main results. The first one is the discovery of two classes of geometric objects called type-α and type-β k-spirals that are preserved under T_k for all $k \geq 2$. These two classes of objects are subsets of *twisted polygons*: bi-infinite sequences $P : \mathbb{Z} \to \mathbb{RP}^2$ such that no three consecutive points are collinear, and $P_{i+n} = \phi(P_i)$ for some fixed projective transformation ϕ called the *monodromy*. The moduli space of projective equivalent twisted n-gons is conventionally denoted by $\mathcal{P}_n$. The type-α and type-β k-spirals are the first discovered classes of geometric constructions of T_k that generalize the pentagram map, which provides crucial evidence for a more general understanding of geometrically preserved classes under T_k.

The second result is the precompactness of both forward and backward T_k-orbits of type-α and type-β k-spirals modulo projective transformations for $k = 2$ and 3, a key property satisfied by convex polygons under the pentagram map discovered by Schwartz

in [Sch92]. We first examine the action of T_3 on type-α and type-β 3-spirals. We show that one can characterize type-α and type-β 3-spirals via linear constraints on the corner invariants. We also derive a birational formula of T_3 for the corner invariants, which is a generalization of the combinatorial formulas developed by [GP16]. Then, we present four global invariants under T_3, which we use to prove the precompactness of T_3-orbits modulo projective transformations. For the case $k = 2$, we show that there exists no type-α 2-spirals and that the type-β 2-spirals are distinct from closed convex polygons. We use the Casimir functions of the T_2-invariant Poisson structure developed in [Sch08] and [OST10] to show that type-β 2-spirals have precompact T_2-orbits modulo projective transformations.

1.2 The k-Spirals under the Map T_k

Here we describe the geometric picture of a k-spiral. For the formal definition, see §3.1. Geometrically, $[P] \in \mathcal{P}_n$ is a *k-spiral* if for all $N \in \mathbb{Z}$, we can find a representative P such that $\{P_i\}_{i \geq N}$ lies on the affine patch, and the triangles (P_i, P_{i+1}, P_{i+2}) and (P_i, P_{i+1}, P_{i+k}) have positive orientation for all $i \geq N$. We call P an *N-representative* of $[P]$.

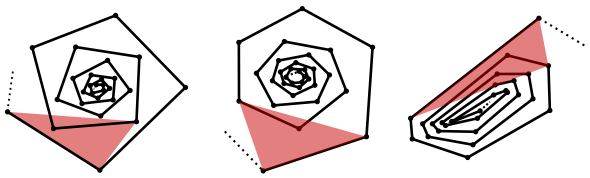

Figure 3: A gallery of 5-spirals. Left: $\mathcal{S}^{\alpha}_{5,3}$. Middle: $\mathcal{S}^{\beta}_{5,3}$. Right: $\mathcal{S}^{\beta}_{5,20}$. The red-shaded triangles indicate the defining orientations and containment relations of type-α and type-β k-spirals..

We are mainly interested in two types of k-spirals, which we term *type-α* and *type-β* (although there certainly exist many more types of spirals, we only consider these two types here). They are k-spirals with additional constraints on the arrangement of the four points $P_i, P_{i+1}, P_{i+k}, P_{i+k+1}$. For type-$\alpha$ spirals, we require P_{i+k} to be contained in the

interior of the triangle $(P_i, P_{i+1}, P_{i+k+1})$. For type-$\beta$ spirals, P_{i+k+1} needs to be contained in the interior of (P_i, P_{i+1}, P_{i+k}). We say P is a *type-α or type-β N-representative*. A class of twisted polygons $[P]$ is a type-α k-spiral (resp. β) if and only if it admits a type-α (resp. β) N-representative for all $N \in \mathbb{Z}$. Let $\mathcal{S}^{\alpha}_{k,n}$ and $\mathcal{S}^{\beta}_{k,n}$ denote the space of type-α and type-β k-spirals modulo projective equivalence. We will see in §3.1 that they are both open in $\mathcal{P}_n$ and hence have dimension $2n$. Figure 3 illustrates three examples of representatives of $\mathcal{S}^{\alpha}_{5,n}$ for $n = 3$, and 20.

It turns out that $\mathcal{S}^{\alpha}_{k,n}$ and $\mathcal{S}^{\beta}_{k,n}$ are invariant under both T_k and T_k^{-1}. Figure 4 shows the inward half of a representative P of $[P] \in \mathcal{S}^{\beta}_{5,3}$, with the red arc representing $P' = T_5(P)$. On the right we have five polygonal arcs by joining vertices of P that are 5 clicks apart. We call them *the transversals of P*. One way to distinguish type-α and type-β spirals is by looking at the orientations of transversals. The transversals of type-α spirals are counterclockwise, whereas those of type-β are clockwise (See Figure 11). In §3, we use the orientations of these transversals to prove the following main theorem.

Theorem 1.1. *For all $n \geq 2$ and $k \geq 2$, we have $T_k(\mathcal{S}^{\alpha}_{k,n}) = \mathcal{S}^{\alpha}_{k,n}$. The same is true for type-β.*

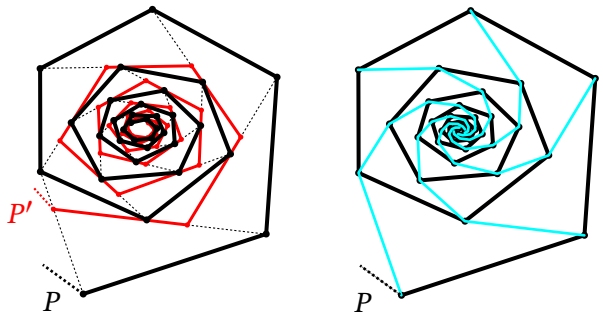

Figure 4: Left: T_5 acting on a representative P of $[P] \in \mathcal{S}^{\beta}_{5,3}$. Right: Transversals of P.

A key property satisfied by convex polygons under the pentagram map is that the forward and backward orbits of any convex polygon under the pentagram map are precompact modulo projective tranformations. See [Sch92, Lemma 3.2]. Experimental results suggest that the k-birds also have precompact Δ_k-orbits. In [Sch25, Conjecture 8.2]

Schwartz conjectured that the k-birds have precompact forward Δ_k-orbits modulo affine transformations. We observed experimentally that $\mathcal{S}^{\alpha}_{k,n}$ and $\mathcal{S}^{\beta}_{k,n}$ behave analogously under T_k.

Conjecture 1.2. *For $n \geq 2$ and $k \geq 2$, the forward and backward T_k-orbit of any $[P] \in \mathcal{S}^{\alpha}_{k,n}$ is precompact in $\mathcal{P}_n$. The same holds for type-β.*

In §6 and §7, we prove Conjecture 1.2 for $k = 2$ and $k = 3$.

1.3 Tic-Tac-Toe Partition and Precompact T_3 Orbits

Our main focus will be the case $k = 3$, which we prove in §6.2.

Theorem 1.3. *For $n \geq 2$, the forward and backward T_3-orbit of any $[P] \in \mathcal{S}^{\alpha}_{3,n}$ is precompact in $\mathcal{P}_n$. The same holds for type-β.*

We discovered several interesting properties of the two types of k-spirals and the map T_3 along our way to prove Theorem 1.3. One major discovery is that the sets $\mathcal{S}^{\alpha}_{3,n}$ and $\mathcal{S}^{\beta}_{3,n}$ fit well with a local parameterization of $\mathcal{P}_n \to \mathbb{R}^{2n}$ introduced by [Sch92] called *corner invariants* (See §2.4). The invariant sets of $\mathcal{P}_n$ under T_3 are partitioned by linear boundaries in the parameter space. The boundary lines give a grid pattern that resembles the board of the game "tic-tac-toe." Each of the four "side-squares" is invariant under T_3.

To construct the tic-tac-toe board, consider the three intervals I, J, K of $\mathbb{R}$ given by $I = (-\infty, 0)$, $J = (0, 1)$, $K = (1, \infty)$. The squares are of the form $I \times I$, $I \times J$, $I \times K$, $J \times I$, etc.. We mark the four side-squares $S_n(I, J)$, $S_n(J, I)$, $S_n(K, J)$, $S_n(J, K)$. See Figure 5 for a visualization of the tic-tac-toe grid. Given $[P] \in \mathcal{P}_n$, we say $[P] \in S_n(I, J)$ if all even corner invariants of $[P]$ are in I, and all odd ones are in J. This means if we plot all n pairs of corner invariants (x_{2i}, x_{2i+1}) onto $\mathbb{R}^2$, we would see n points lying in $I \times J$. The other three side squares are defined analogously.

Figure 6 shows vertices of a representative P of $[P] \in S_4(K, J)$ and the image $P' = T_3(P)$. On the right, we have the projection of the first 2^{11} iterations of the orbit of P under T_3. Each point corresponds to $P_3^{(m)}$ after normalizing $(P_{-2}^{(m)}, P_{-1}^{(m)}, P_0^{(m)}, P_1^{(m)})$ to the unit square

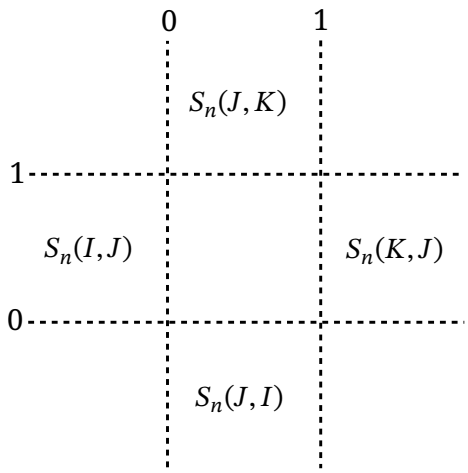

Figure 5: The partition of $\mathbb{R}^2$ into a 3×3 grid, and the four side-squares of our interest.

(here $P^{(m)} = T_3^m(P)$). We speculate that the orbit lies on a flat torus, where the map T_3 acts as a translation on the flat metric.

Twisted polygons that are assigned to these squares have geometric properties. For example, the closed convex polygons always lie in the center square; two of the side-squares are $\mathcal{S}^{\alpha}_{3,n}$ and $\mathcal{S}^{\beta}_{3,n}$; the other two side-squares are obtained by reverting the indexing of vertices of these two types of k-spirals. These facts will be proved in §4.

The proof of Theorem 1.3 is algebraic. In §5 I show that T_3 is a birational map on the corner invariants, which generalizes a direct application of [GP16, Theorem 1.6]. For the explicit formulas, see Equation (19). In §6, I derive four algebraic invariants of T_3, which allow me to show boundedness of the corner invariants of the T_3-orbits, thereby proving Theorem 1.3. This approach is reminiscent of Schwartz's second proof of precompactness of T_2-orbits of convex polygons in [Sch01, Section 3B & 3C].

1.4 The Type-β 2-Spirals and Precompact T_2 Orbits

We now proceed to the case $k = 2$, where the map T_2 is the classical pentagram map. In §3.1 we show that there exist no type-α 2-spirals (so Conjecture 1.2 is vacuously true for type-α 2-spirals). On the other hand, type-β 2-spirals are nontrivial geometric constructions that

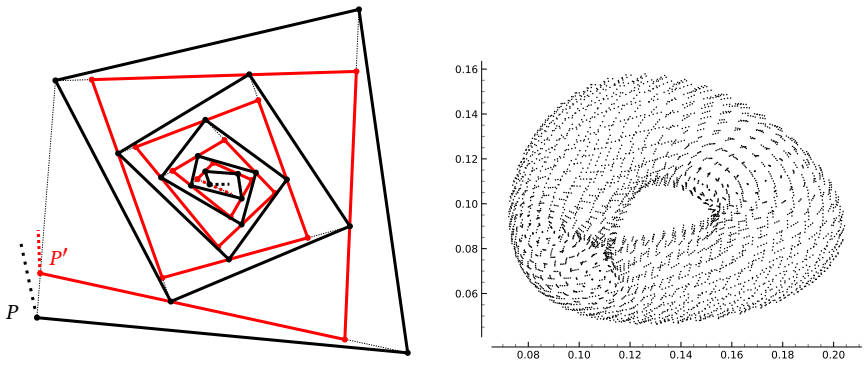

Figure 6: Left: T_3 acting on a representative of $[P] \in S_4(K,J)$. Right: The orbit of $P_3^{(m)}$ in $\mathbb{A}^2$ by fixing $P_{-2} = (0,0)$, $P_{-1} = (1,0)$, $P_0 = (1,1)$, $P_1 = (0,1)$.

are distinct from convex polygons. In §7.1, we show that the corner invariants of type-β 2-spirals are also partitioned by linear boundaries, and in particular $\mathcal{S}^{\alpha}_{3,n} \subset \mathcal{S}^{\beta}_{2,n}$.

We point out that the type-β 2-spirals are not related to the pentagram spirals in [Sch13]. The latter requires P to be a relabeling of $T_2^m(P)$ for some positive integer m.

In §7.2, we use the Casimir functions of the T_2-invariant Poisson structure on $\mathcal{P}_n$ from [Sch08] and [OST10] to prove Conjecture 1.2 for $k = 2$.

Theorem 1.4. *For $n \geq 2$, the forward and backward T_2-orbit of any $[P] \in \mathcal{S}^{\beta}_{2,n}$ is precompact in $\mathcal{P}_n$.*

1.5 Obstacles for $k > 3$ and Future Directions

Our algebraic method of proving Theorem 1.3 and 1.4 requires a complete characterization of the corner invariants of $\mathcal{S}^{\alpha}_{k,n}$ and $\mathcal{S}^{\beta}_{k,n}$ and enough algebraic invariants of T_k that uniformly bound the corner invariants away from the boundaries of $\mathcal{S}^{\alpha}_{k,n}$ and $\mathcal{S}^{\beta}_{k,n}$. However, the corner invariants seem to be not partitioned by linear boundaries for $k > 3$, which makes it difficult to analyze the boundaries of the corner invariants of $\mathcal{S}^{\alpha}_{k,n}$ and $\mathcal{S}^{\beta}_{k,n}$. Moreover, the map T_k for the corner invariants seems not birational from computer algebra. This makes it difficult to algebraically characterize the corner invariants.

One future direction is to look at the cross-ratio of different combinations of points other than the ones involved in the definition of corner invariants. In §8 we present a conjecture on a potential algebraic invariant of T_k, which can be interpreted as a Casimir function of a Poisson structure over the y-parameteris of a quiver Q_S. The quiver Q_S is associated to a Y-mesh of type S from [GP16] and is isomorphic to the quiver in [GSTV12], which corresponds geometrically to the map T_k.

Another direction is to analyze the two types of k-spirals geometrically. There are yet many open problems on the geometry of the two types of k-spirals that could hint at the behavior of their T_k-orbits. For open problems, see the end of §3.1. Answering these geometric problems may provide a new approach to tackle Conjecture 1.2.

Finally, for the case $k = 3$, the birational formula for T_3 could be applied to other settings such as the action of T_3 on Poncelet polygons [Sch24] or discovering T_3-compatible Poisson structures on $\mathcal{P}_n$ that generalizes the one in [GSTV12] for corrugated polygons.

1.6 Accompanying Program

I wrote a web-based program to visualize the orbits of twisted polygons under T_k. Readers can access it from the following link:

https://zzou9.github.io/pentagram-map/spiral.html

When reaching the website, you will see a representative of a twisted polygon displayed in the middle of the screen. You can click on the user manual button for instructions on how to use the program. I discovered most of the results by computer experiments using this program. The paper contains rigorous proofs of the beautiful pictures I observed from it.

1.7 Acknowledgements

This work was supported by a Brown University SPRINT/UTRA summer research program grant. I would like to thank my advisor, Richard Evan Schwartz, for introducing

the concept of deep diagonal maps, providing extensive insights throughout the project, and offering guidance during the writing process. I would like to thank Anton Izosimov and Sergei Tabachnikov for their insightful discussions on the tic-tac-toe partition. Finally, I am grateful to the referees for their helpful comments and for highlighting the connections between the birational formula and the work of Glick and Pylyavskyy.

2 Background

2.1 Projective Geometry

The real projective plane $\mathbb{RP}^2$ is the space of 1-dimensional subspaces of $\mathbb{R}^3$. *Points* of $\mathbb{RP}^2$ are lines in $\mathbb{R}^3$ that go through the origin. We say that $[x : y : z]$ is a *homogeneous coordinate* of $V \in \mathbb{RP}^2$ if the vector $\tilde{V} = (x, y, z)$ is a representative of V. Given two distinct points $V_1, V_2 \in \mathbb{RP}^2$, the *line* $l = V_1V_2$ connecting V_1 and V_2 is the 2-dimensional hyperplane spanned by the two 1-dimensional subspaces. Let l_1, l_2 be two lines in $\mathbb{RP}^2$. The *point of intersection* $l_1 \cap l_2$ is the 1-dimensional line given by the intersection of the two 2-dimensional subspaces. In $\mathbb{RP}^2$, there exists a unique line connecting each pair of distinct points and a unique point of intersection given two distinct lines. We call a collection of points $V_1, V_2, \dots, V_n \in \mathbb{RP}^2$ *in general position* if no three of them are collinear.

The *affine patch* $\mathbb{A}^2$ consists of points in $\mathbb{RP}^2$ with homogeneous coordinate $[x : y : 1]$. We call this canonical choice of coordinate $(x, y, 1)$ the *affine coordinate* of a point $V \in \mathbb{A}^2$. There is a diffeomorphism $\Phi : \mathbb{R}^2 \to \mathbb{A}^2$ given by $\Phi(x, y) = [x : y : 1]$. We often identify $\mathbb{A}^2$ as a copy of $\mathbb{R}^2$ in $\mathbb{RP}^2$. The line $\mathbb{RP}^2 - \mathbb{A}^2$ is called the *line at infinity*.

A map $\phi : \mathbb{RP}^2 \to \mathbb{RP}^2$ is a *projective transformation* if it maps points to points and lines to lines and is bijective. Algebraically, the group of projective transformations is $\mathrm{PGL}_3(\mathbb{R}) = \mathrm{GL}_3(\mathbb{R})/\mathbb{R}^*I$, where we are modding by the subgroup $\mathbb{R}^*I = \{\lambda I : \lambda \in \mathbb{R}^*\}$ and I is the 3×3 identity matrix. We state a classical result regarding projective transformations below with its proof omitted.

Theorem 2.1. *Given two 4-tuples of points* (V_1, V_2, V_3, V_4) *and* (W_1, W_2, W_3, W_4) *in* $\mathbb{RP}^2$*, both in general position, there exists a unique* $\phi \in \mathrm{PGL}_3(\mathbb{R})$ *such that* $\phi(V_i) = W_i$*.*

The group of *affine transformations* $\mathrm{Aff}_2(\mathbb{R})$ on $\mathbb{A}^2$ is the subgroup of projective transformations that fixes the line at infinity. It is isomorphic to a semidirect product of $\mathrm{GL}_2(\mathbb{R})$ and $\mathbb{R}^2$. Elements of $\mathrm{Aff}_2(\mathbb{R})$ can be uniquely expressed as a tuple (M', v) where $M' \in \mathrm{GL}_2(\mathbb{R})$ and $v \in \mathbb{R}^2$. Let $\mathrm{Aff}_2^+(\mathbb{R})$ denote the subgroup of $\mathrm{Aff}_2^+(\mathbb{R})$ where $(M', v) \in \mathrm{Aff}_2^+(\mathbb{R})$ iff $\det(M') > 0$. These are orientation-preserving affine transformations.

2.2 Orientation of Affine Triangles

Given an ordered 3-tuple (V_1, V_2, V_3) of points in $\mathbb{R}^2$ or $\mathbb{A}^2$, let $\mathrm{int}(V_1, V_2, V_3)$ denote the interior of the affine triangle with vertices V_1, V_2, V_3. There is a canonical way to define the orientation of an ordered 3-tuple. Let $\tilde{V}_i$ be the affine coordinate of V_i. We consider the *signed area* $\mathcal{O}(V_1, V_2, V_3)$ of the oriented triangle, which can be computed as

$$\mathcal{O}(V_1, V_2, V_3) = \det(\tilde{V}_1, \tilde{V}_2, \tilde{V}_3). \tag{2}$$

The determinant is evaluated on the 3×3 matrix with column vectors $\tilde{V}_i$. We say an ordered 3-tuple (V_1, V_2, V_3) is *positive* if $\mathcal{O}(V_1, V_2, V_3) > 0$. Figure 7 shows an example of a positive 3-tuple.

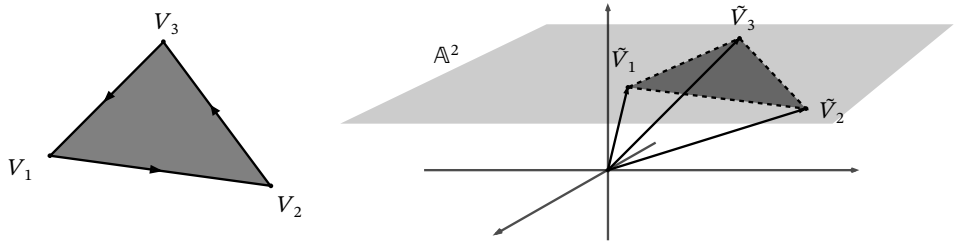

Figure 7: A positive 3-tuple of affine points (V_1, V_2, V_3).

Here is another way to compute $\mathcal{O}$ using the $\mathbb{R}^2$ coordinates of V_1, V_2, V_3:

$$\begin{aligned}\mathcal{O}(V_1, V_2, V_3) &= \det(V_1, V_2) + \det(V_2, V_3) + \det(V_3, V_1) \\ &= \det(V_i - V_{i-1}, V_{i+1} - V_i) \text{ for } i = 1, 2, 3\end{aligned} \tag{3}$$

where the determinant is evaluated on the 2×2 matrix.

$\mathcal{O}$ interacts with the action of $\mathrm{Aff}_2^+(\mathbb{R})$ and the symmetric group S_3 on planar/affine triangles in the following way: Given $M \in \mathrm{Aff}_2^+(\mathbb{R})$, let $V_i' = M(V_i)$. One can show that (V_1, V_2, V_3) is positive iff (V_1', V_2', V_3') is positive. On the other hand, for all $\sigma \in S_3$, $\mathcal{O}(V_{\sigma(1)}, V_{\sigma(2)}, V_{\sigma(3)}) = \mathrm{sgn}(\sigma)\mathcal{O}(V_1, V_2, V_3)$, so $\mathcal{O}(V_{\sigma(1)}, V_{\sigma(2)}, V_{\sigma(3)}) = \mathcal{O}(V_1, V_2, V_3)$ when σ is a 3-cycle.

Below are useful equivalence conditions for the positivity of (V_1, V_2, V_3). The proof is elementary, so we will omit it.

Proposition 2.2. *Given $V_1, V_2, V_3 \in \mathbb{R}^2$ in general position, and $W \in \mathrm{int}(V_1, V_2, V_3)$, the following are equivalent:*

1. *(V_1, V_2, V_3) is positive.*
2. *(V_i, V_{i+1}, W) is positive for some $i \in \{1, 2, 3\}$.*
3. *(V_i, V_{i+1}, W) is positive for all $i \in \{1, 2, 3\}$.*
4. *$\det(V_i - V_{i-1}, V_{i+1} - W) > 0$ for some $i \in \{1, 2, 3\}$.*
5. *$\det(V_i - V_{i-1}, V_{i+1} - W) > 0$ for all $i \in \{1, 2, 3\}$.*

2.3 The Cross-Ratio

The cross-ratio is used to construct a projective-invariant parametrization of the k-spirals. There are multiple ways to define the cross-ratio of four collinear points on the projective plane, each using its own permutation of the points. We follow the convention used in [Sch92]. Given four collinear points A, B, C, D on a line $\omega \subset \mathbb{RP}^2$, we choose a projective

transformation ψ that maps ω to the x-axis of $\mathbb{A}^2$. Let a, b, c, d be the x-coordinates of $\psi(A)$, $\psi(B)$, $\psi(C)$, $\psi(D)$. We define the *cross-ratio* to be the following quantity:

$$\chi(A, B, C, D) := \frac{(a-b)(c-d)}{(a-c)(b-d)}. \tag{4}$$

If A lies on the line at infinity, we let $\chi(A, B, C, D) = \frac{c-d}{b-d}$. One can check that given any $\phi \in \mathrm{PGL}_3(\mathbb{R})$,

$$\chi(A, B, C, D) = \chi(\phi(A), \phi(B), \phi(C), \phi(D)).$$

We also define the cross-ratio for four projective lines. Let l, m, n, k be four lines intersecting at a common point O. Normalize with a projective transformation so that $l, m, n, k \subset \mathbb{A}^2$ with slopes s_l, s_m, s_n, s_k. We define

$$\chi(l, m, n, k) = \frac{(s_l - s_m)(s_n - s_k)}{(s_l - s_n)(s_m - s_k)} \tag{5}$$

with $\chi(l, m, n, k) = \frac{s_n - s_k}{s_m - s_k}$ if $s_l = \infty$.

If ω is a line that does not go through O and intersects l, m, n, k at A, B, C, D respectively, we have

$$\chi(l, m, n, k) = \chi(A, B, C, D). \tag{6}$$

See Figure 8 for the configuration. The proof is elementary, so we will omit it.

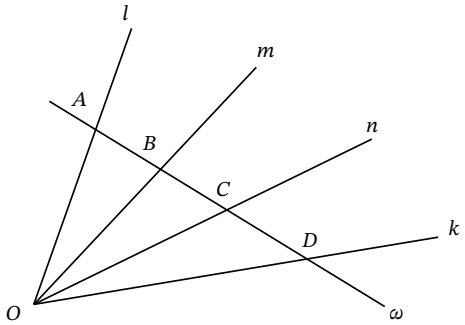

Figure 8: The configuration in Equation (6).

2.4 Twisted Polygons, Corner Invariants

Introduced in [Sch08], a *twisted n-gon* is a bi-infinite sequence $P : \mathbb{Z} \to \mathbb{RP}^2$, along with a projective transformation $M \in \mathrm{PGL}_3(\mathbb{R})$ called the *monodromy*, such that every three consecutive points of P are in general position, and $P_{i+n} = M(P_i)$ for all $i \in \mathbb{Z}$. When M is the identity, we get an ordinary closed n-gon. Two twisted n-gons P, Q are *equivalent* if there exists $\phi \in \mathrm{PGL}_3(\mathbb{R})$ such that $\phi(P_i) = Q_i$ for all $i \in \mathbb{Z}$. The two monodromies M_p and M_q satisfy $M_q = \phi M_p \phi^{-1}$. Let $\mathcal{P}_n$ denote the space of twisted n-gons modulo projective equivalence.

The cross-ratio allows us to parameterize $\mathcal{P}_n$ with coordinates in $\mathbb{R}^{2n}$. Given a twisted n-gon P, the *corner invariants* of P is a coordinate system $x_0(P), \dots, x_{2n-1}(P)$ given by

$$\begin{cases} x_{2i}(P) = \chi(P_{i-2},\, P_{i-1},\, P_{i-2}P_{i-1} \cap P_iP_{i+1},\, P_{i-2}P_{i-1} \cap P_{i+1}P_{i+2}); \\ x_{2i+1}(P) = \chi(P_{i+2},\, P_{i+1},\, P_{i+2}P_{i+1} \cap P_iP_{i-1},\, P_{i+2}P_{i+1} \cap P_{i-1}P_{i-2}). \end{cases} \tag{7}$$

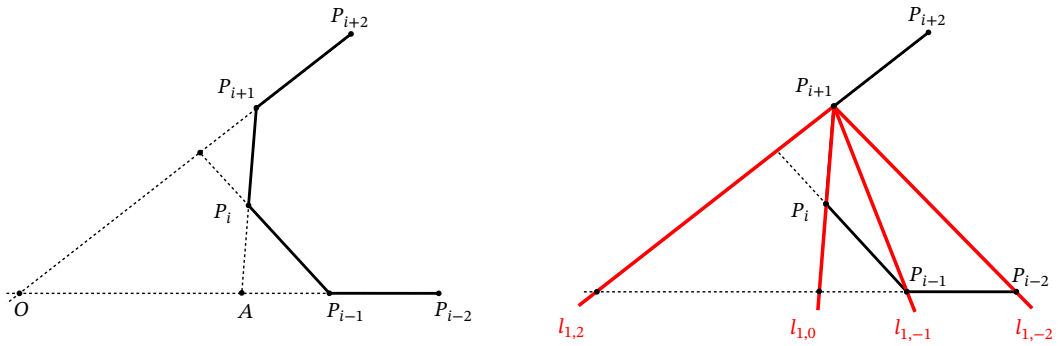

Figure 9: Left: The corner invariants $x_{2i}(P) = \chi(P_{i-2}, P_{i-1}, A, O)$ computed using Equation (7). Right: $x_{2i}(P) = \chi(l_{1,-2}, l_{1,-1}, l_{1,0}, l_{1,2})$ computed using Equation (8).

See the left side of Figure 9 for a geometric interpretation of the corner invariants. Let $l_{a,b} = P_{i+a}P_{i+b}$. By Equation (5), the corner invariants can be computed by

$$\begin{cases} x_{2i}(P) = \chi(l_{1,-2}, l_{1,-1}, l_{1,0}, l_{1,2}); \\ x_{2i+1}(P) = \chi(l_{-1,2}, l_{-1,1}, l_{-1,0}, l_{-1,-2}). \end{cases} \tag{8}$$

See the right side of Figure 9 for the line configurations.

Since χ is invariant under projective transformations, for all j we have $x_j(P) = x_{j+2n}(P)$, so a $2n$-tuple of corner invariants is enough to fully determine the projective equivalence class of a twisted n-gon. We use $x_j(P)$ to denote the corner invariants of $[P] \in \mathcal{P}_n$ without adding square brackets around P. To obtain the corner invariants of $[P] \in \mathcal{P}_n$, one can simply choose an arbitrary representative P and compute its corner invariants. [Sch08, Equation (19) & (20)] showed that one can also revert the process and obtain a representative twisted polygon of the equivalence class given its corner invariants.

3 The Spirals and T_k-Orbit Invariance

In this section, we explore the geometric properties of type-α and type-β k-spirals and prove Theorem 1.1. In §3.1, we give rigorous definitions of the two types of k-spirals and discuss their geometric properties. In §3.2, we introduce a construct associated to the two types of k-spirals called the transversals. In §3.3 and §3.4, we prove Theorem 1.1 using geometric properties of the transversals.

3.1 The Geometry of k-Spirals

Here we give the formal definition of a k-spiral and its two subsets called type-α and type-β. We then explore their geometric properties and present some open problems.

Definition 3.1. Given integers $k \geq 2$, $n \geq 2$, we say that $[P] \in \mathcal{P}_n$ is a *k-spiral* if for all $N \in \mathbb{Z}$, there exists a representative P that satisfies the following: For all $i \geq N$, P_i lies in $\mathbb{A}^2$, (P_i, P_{i+1}, P_{i+2}) is positive, and (P_i, P_{i+1}, P_{i+k}) is positive. Such a representative is called an *N-representative*. Saying that $[P]$ is a k-spiral means that $[P]$ admits an N-representative for all $N \in \mathbb{Z}$.

Remark 3.2. The idea of considering an N-representative for each $N \in \mathbb{Z}$ is new to the literature and may at first seem superfluous. Readers will see in §4 that this condition is natural when we examine the corner invariants of the two types of k-spirals. See the end of this section for open problems related to the geometry of N-representatives.

In practice, since $[P]$ is a twisted n-gon, it suffices to find a single N_0-representative P_0 for some $N_0 \in \mathbb{Z}$. One can then obtain other N-representatives for $N < N_0$ by applying the m-th power of the monodromy of $[P]$ to P_0, where $m > \frac{N_0 - N}{k} + 1$.

Definition 3.3. A k-spiral $[P] \in \mathcal{P}_n$ is of *type-α* or *type-β* if for all $N \in \mathbb{Z}$, it has an N-representative P that satisfies the following conditions:

- $[P]$ is of type-α if $P_{i+k} \in \operatorname{int}(P_i, P_{i+1}, P_{i+k+1})$ for all $i \geq N$;
- $[P]$ is of type-β if $P_{i+k+1} \in \operatorname{int}(P_i, P_{i+1}, P_{i+k})$ for all $i \geq N$.

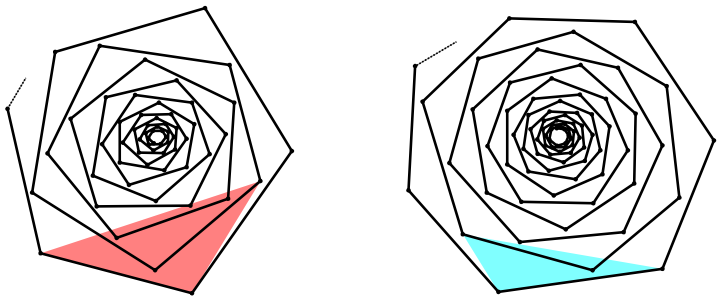

Figure 10: Left: The inward half of a 0-representative P of a type-α 6-spiral. The red triangle is joined by $(P_i, P_{i+1}, P_{i+k+1})$, which is positive by Proposition 3.4 and contains P_{i+k} in its interior. Right: The inward half of a 0-representative P of a type-β 6-spiral. The cyan triangle is joined by (P_i, P_{i+1}, P_{i+k}), which is positive and contains P_{i+k+1} in its interior.

See Figure 10 for 0-representatives of type-α and type-β 6-spirals. For the type-α k-spirals, we show that positivity of (P_i, P_{i+1}, P_{i+k}) is equivalent to positivity of $(P_i, P_{i+1}, P_{i+k+1})$. The latter condition turns out to be more convenient for showing T_k invariance.

Proposition 3.4. *$[P] \in \mathcal{P}_n$ is a type-α k-spiral if and only if for all $N \in \mathbb{Z}$, there exists a representative P that satisfies the following: for all $i \geq N$, P_i lies in $\mathbb{A}^2$, (P_i, P_{i+1}, P_{i+2}) is positive, $(P_i, P_{i+1}, P_{i+k+1})$ is positive, and $P_{i+k} \in \operatorname{int}(P_i, P_{i+1}, P_{i+k+1})$.*

Proof. Since $P_{i+k} \in \operatorname{int}(P_i, P_{i+1}, P_{i+k+1})$, we see that $\operatorname{int}(P_i, P_{i+1}, P_{i+k+1})$ is nonempty, so the three points P_i, P_{i+1}, P_{i+k+1} are in general position. It then follows from Proposition 2.2 that (P_i, P_{i+1}, P_{i+k}) is positive iff $(P_i, P_{i+1}, P_{i+k+1})$ is positive. □

Corollary 3.5. *There exists no type-α 2-spirals.*

Proof. It suffices to show that there exists no configuration of four points $A, B, C, D \in \mathbb{A}^2$ such that (A, B, D), (B, C, D) are both positive and $C \in \operatorname{int}(A, B, D)$. If (A, B, D) is positive and $C \in \operatorname{int}(A, B, D)$, then Proposition 2.2 implies (B, D, C) is positive, but that contradicts (B, C, D) positive because $\mathcal{O}(B, C, D) = -\mathcal{O}(B, D, C)$. □

On the other hand, type-β 2-spirals do exist. Geometrically, their N-representatives look like triangular spirals. See §7 for a more thorough discussion on type-β 2-spirals.

Remark 3.6. One may attempt to define the two types of k-spirals on bi-infinite sequences of points in $\mathbb{RP}^2$ with no periodicity constraints. The results in this section hold true for this more general definition. We restrict our attention to twisted polygons because it's a finite-dimensional space, which allows us to more easily keep track of the T_k-orbits.

We now proceed to discuss some geometric properties of type-α and type-β k-spirals. A twisted polygon P is called *k-nice* if the four points $P_i, P_{i+1}, P_{i+k}, P_{i+k+1}$ are in general position for all $i \in \mathbb{Z}$. The k-nice condition is projective invariant. Let $\mathcal{P}_{k,n}$ denote the space of k-nice twisted n-gons modulo projective equivalence.

Proposition 3.7. *For all $k \geq 2$, $\mathcal{P}_{k,n}$ is open in $\mathcal{P}_n$, so it has dimension $2n$.*

Proof. The condition that four points $P_i, P_{i+1}, P_{i+k}, P_{i+k+1}$ are in general position remains true if we perturb one of the points in a small enough neighborhood of $\mathbb{RP}^2$. The dimension of $\mathcal{P}_{k,n}$ comes from the fact that $\mathcal{P}_n$ has dimension $2n$, which is shown in [OST10, Lemma 2.2]. □

Proposition 3.8. *Both type-α and type-β k-spirals are k-nice.*

Proof. We give a proof to the type-α case. The type-β case is analogous, so we will omit it. Given a type-α k-spiral $[P]$ and an integer $i \in \mathbb{Z}$, let P be an i-representative of $[P]$. Since $(P_i, P_{i+1}, P_{i+k+1})$ is positive, these three points cannot be collinear. Also, since $P_{i+k} \in \operatorname{int}(P_i, P_{i+1}, P_{i+k+1})$, P_{i+k} does not lie in any of the lines joined by two of the three vertices P_i, P_{i+1}, P_{i+k+1}. This shows that $P_i, P_{i+1}, P_{i+k}, P_{i+k+1}$ are in general position. □

As stated in §1.2, we let $\mathcal{S}^{\alpha}_{k,n}$ and $\mathcal{S}^{\beta}_{k,n}$ denote the space of type-α and type-β k-spirals (By Corollary 3.5, $\mathcal{S}^{\alpha}_{2,n} = \emptyset$ for all $n \geq 2$).

Proposition 3.9. *Both $\mathcal{S}^{\alpha}_{k,n}$ and $\mathcal{S}^{\beta}_{k,n}$ are open in $\mathcal{P}_{k,n}$, so they both have dimension $2n$.*

Proof. The positivity conditions of (P_i, P_{i+1}, P_{i+2}) and (P_i, P_{i+1}, P_{i+k}) are open conditions from continuity of the determinant function. The condition $P_{i+k} \in \mathrm{int}(P_i, P_{i+1}, P_{i+k+1})$ for type-α (or $P_{i+k+1} \in \mathrm{int}(P_i, P_{i+1}, P_{i+k})$ for type-β) is equivalent to the positivity of certain determinants by Proposition 2.2, so this is also an open condition. Finally, $\mathcal{S}^{\alpha}_{k,n} \subset \mathcal{P}_{k,n}$ and $\mathcal{S}^{\beta}_{k,n} \subset \mathcal{P}_{k,n}$ follows from Proposition 3.8. □

A twisted polygon P is *closed* if there exists some positive integer n such that $P_{i+n} = P_i$, or $[P] \in \mathcal{P}_n$ with identity monodromy. We show that neither type-α nor type-β k-spirals are closed.

Proposition 3.10. *For all $k \geq 2$ and $n \geq 2$, if $[P] \in \mathcal{S}^{\alpha}_{k,n}$, then $[P]$ is not closed. The same holds for $\mathcal{S}^{\beta}_{k,n}$.*

Proof. Given any closed n-gon P on $\mathbb{A}^2$, let C be the convex hull of the vertices of P. Since P has finitely many vertices, there exists a vertex P_i such that $P_i \notin \mathrm{int}(C)$. Then, since $\mathrm{int}(P_{i-k}, P_{i-k+1}, P_{i+1}) \subset \mathrm{int}(C)$, we must have $P_i \notin \mathrm{int}(P_{i-k}, P_{i-k+1}, P_{i+1})$. It follows that P is not an N-representative of type-α k-spiral for any N or k. The proof for type-β is similar, so we omit it. □

The two types of k-spirals seem to possess rich geometric properties. We will present some open problems. In the discussion below, $[P]$ denotes a type-α or type-β k-spiral.

Problem 3.11. For all $N \in \mathbb{Z}$, is it always possible to find N-representatives P such that for all $j > i + 1$, (P_i, P_{i+1}, P_j) is positive (in other words, P_j always lies on the same side of the line P_iP_{i+1})?

Problem 3.12. Let P be an arbitrary representative of $[P]$. Is there a minimal $N \in \mathbb{Z}$ such that P is an N-representative on some affine patch of $\mathbb{RP}^2$? Does there exist P that is an N-representative for all $N \in \mathbb{Z}$?

Problem 3.13. Given an N-representative P, does P_i converge to a point in $\mathbb{A}^2$ as $i \to \infty$?

3.2 Transversals of the Spirals

In this section, we prove our remark in §1.2 that transversals for type-α spirals are oriented counterclockwise, whereas transversals for type-β are oriented clockwise. Recall that the *transversals* of an N-representative P of a k-spiral are k polygonal arcs joined by vertices $P_i, P_{i+k}, P_{i+2k}, \ldots$ for $i = N, \ldots, N+k-1$. See Figure 11 for one of the k transversals of the two representatives from Figure 10.

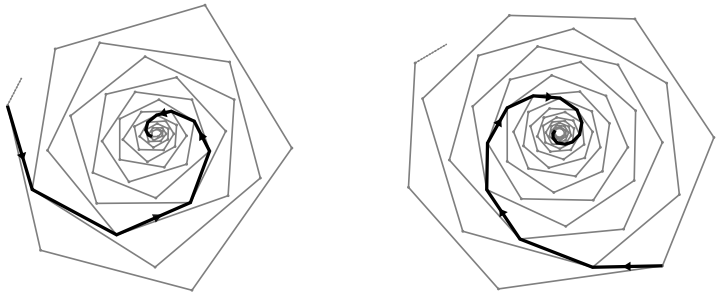

Figure 11: Transversals of two representatives from Figure 10.

Lemma 3.14. *Given $O, A, B, C, D \in \mathbb{A}^2$ (See Figure 12) such that (A,O,B), (A,O,D), (B,O,C), (C,O,D) are all positive. Then, (A,O,C) is positive iff (B,O,D) is positive.*

Proof. For the forward direction, normalize with $\mathrm{Aff}_2^+(\mathbb{R})$ so that $O = (0,0)$ and $A = (-1,0)$. Let $B = (x_b, y_b)$, $C = (x_c, y_c)$, and $D = (x_d, y_d)$. Since (A,O,B) is positive, Equation (3) gives us

$$\mathcal{O}(A,O,B) = \det(O-A, B-O) = \det(-A,B) = y_b > 0.$$

Similarly, positivity of (A,O,C) and (A,O,D) give us $y_c, y_d > 0$. Next, observe that

$$\mathcal{O}(B,O,C) = \det(-B,C) = -x_b y_c + x_c y_b;$$

$$\mathcal{O}(B,O,D) = \det(-B,D) = -x_b y_d + x_d y_b;$$

$$\mathcal{O}(C,O,D) = \det(-C,D) = -x_c y_d + x_d y_c.$$

Since $y_b, y_c, y_d > 0$, we have $\frac{y_b}{y_c}, \frac{y_d}{y_c} > 0$, which implies

$$\mathcal{O}(B,O,D) = -x_b y_d + x_d y_b = \frac{y_b}{y_c}\,\mathcal{O}(C,O,D) + \frac{y_d}{y_c}\,\mathcal{O}(B,O,C) > 0.$$

This shows positivity of (B,O,D).

The proof for the backward direction is analogous. Normalize so that $O = (0,0)$ and $D = (1,0)$. Let $A = (x_a, y_a)$, $B = (x_b, y_b)$, $C = (x_c, y_c)$. Positivity of (A,O,D), (B,O,D), and (C,O,D) implies $y_a, y_b, y_c > 0$. One can then check that

$$\mathcal{O}(A,O,C) = -x_a y_c + x_c y_a = \frac{y_c}{y_b}\,\mathcal{O}(A,O,B) + \frac{y_a}{y_b}\,\mathcal{O}(B,O,C) > 0.$$

This shows positivity of (A,O,C). □

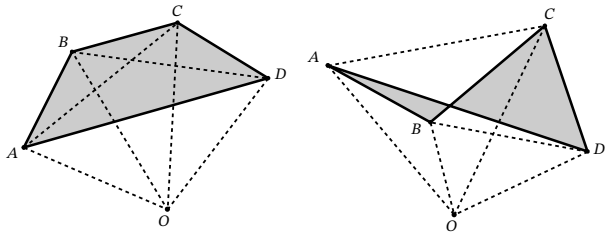

Figure 12: Examples of O, A, B, C, D in Lemma 3.14.

The next proposition formalizes our claim on the orientation of transversals.

Proposition 3.15. *Let P be an N-representative of a k-spiral $[P]$. For all $i > N$, if $[P]$ is type-α, then (P_i, P_{i+k}, P_{i+2k}) is positive; if $[P]$ is type-β, then (P_{i+2k}, P_{i+k}, P_i) is positive.*

Proof. The proof applies Lemma 3.14 with suitable choices of O, A, B, C, D. See Figure 13 for the configuration of points involved.

We start with P of type-α. Consider the following choices of vertices:

$$O = P_{i+k};\ A = P_i;\ B = P_{i+k-1};\ C = P_{i+2k};\ D = P_{i+k+1}.$$

It follows immediately from the definition of a type-α N-representative that (B,O,C) and (B,O,D) are positive. The other conditions follow from applications of Proposition

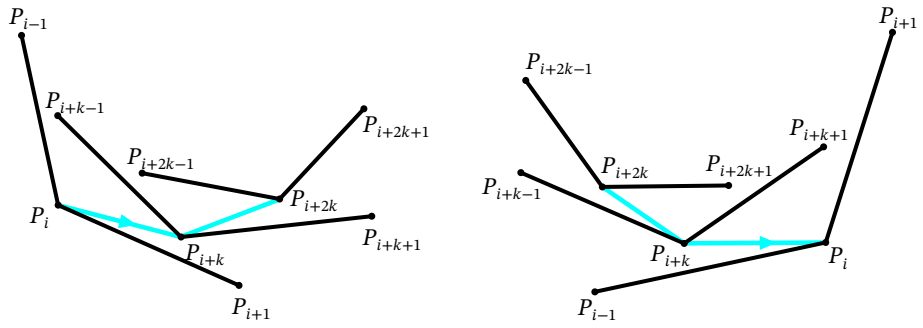

Figure 13: Left: $\mathcal{S}^{\alpha}_{k,n}$ configuration. Right: $\mathcal{S}^{\beta}_{k,n}$ configuration.

2.2. Apply Proposition 2.2 with (P_{i-1}, P_i, P_{i+k}) positive and $P_{i+k-1} \in \text{int}(P_{i-1}, P_i, P_{i+k})$ to get positivity of (A, O, B). Apply Proposition 2.2 with $(P_i, P_{i+1}, P_{i+k+1})$ positive and $P_{i+k} \in \text{int}(P_i, P_{i+1}, P_{i+k+1})$ to get positivity of (A, O, D). Apply Proposition 2.2 with $(P_{i+k}, P_{i+k+1}, P_{i+2k+1})$ positive and $P_{i+2k} \in \text{int}(P_{i+k}, P_{i+k+1}, P_{i+2k+1})$ to get positivity of (C, O, D). Then, the backward direction of Lemma 3.14 implies (P_i, P_{i+k}, P_{i+2k}) is positive.

The proof for type-β is analogous. Consider the following choices of vertices:

$$O = P_{i+k};\ A = P_{i+k-1};\ B = P_{i+2k};\ C = P_{i+k+1};\ D = P_i.$$

Positivity of (A, O, C) and (B, O, C) follows from the definition of a type-β N-representative. A similar application of Proposition 2.2 as in the case of type-α gives positivity of (A, O, B), (A, O, D), and (C, O, D), which we will omit. Finally, the forward direction of Lemma 3.14 implies (P_{i+2k}, P_{i+k}, P_i) is positive. □

3.3 Invariance of Forward Orbit

In this section, we prove that $\mathcal{S}^{\alpha}_{k,n}$ and $\mathcal{S}^{\beta}_{k,n}$ are T_k-invariant. We will use Equation (1) for our labeling convention. See Figure 14.

If P is k-nice, then P' is always well-defined. In particular, Proposition 3.8 implies T_k is well-defined on $\mathcal{S}^{\alpha}_{k,n}$ and $\mathcal{S}^{\beta}_{k,n}$.

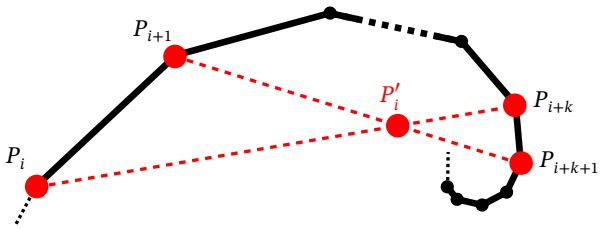

Figure 14: The labeling convention of the map T_k from Equation (1).

Remark 3.16. T_k doesn't necessarily send k-nice twisted polygons to k-nice twisted polygons. Here is an example provided by the anonymous referee: Fix $r \in (0,1)$. Consider the function $P : \mathbb{Z} \to \mathbb{C} \cong \mathbb{R}^2$ mapping $z \mapsto r^z \exp(z\pi i/k)$. One can check that P is a k-nice twisted n-gon for any $n \geq 2$ with monodromy that is a scale-rotation, but $T_k(P)$ is the zero function and hence not k-nice. What we will show is that in the case of type-α and type-β k-spirals, T_k does preserve k-niceness. This is a direct consequence of Theorem 1.1 and Proposition 3.8.

We proceed to prove the T_k-invariance of $\mathcal{S}^{\alpha}_{k,n}$ and $\mathcal{S}^{\beta}_{k,n}$ separately. We start with the following lemma.

Lemma 3.17. *Given four points A, B, C, D in $\mathbb{R}^2$ in general position with $D \in \text{int}(A,B,C)$. Let $O = AB \cap CD$. There exist $s \in (0,1)$ and $t \in (1,\infty)$ such that*

$$O = (1-s)A + sB = (1-t)C + tD.$$

Proof. Since $D \in \text{int}(A,B,C)$, there exists $\lambda_1, \lambda_2, \lambda_3 \in (0,1)$ such that

$$\lambda_1 + \lambda_2 + \lambda_3 = 1; \;\; D = \lambda_1 A + \lambda_2 B + \lambda_3 C.$$

Taking $s = \frac{\lambda_2}{1-\lambda_3}$ and $t = \frac{1}{1-\lambda_3}$ gives us the desired result. □

Proposition 3.18. *For all $k \geq 2$ and $n \geq 2$, $T_k(\mathcal{S}^{\alpha}_{k,n}) \subset \mathcal{S}^{\alpha}_{k,n}$.*

Proof. Given an N-representative P of some $[P] \in \mathcal{S}^{\alpha}_{k,n}$, we will show that $P' = T_k(P)$ is a type-α N-representative of $[T_k(P)]$ by proving that for all $i \geq N$, $(P'_i, P'_{i+1}, P'_{i+2})$ is positive,

$(P'_i, P'_{i+1}, P'_{i+k+1})$ is positive, and $P'_{i+k} \in \operatorname{int}(P'_i, P'_{i+1}, P'_{i+k+1})$. See the left side of Figure 15 for configurations of relevant vertices of P and P'.

Let $i \geq N$ be fixed. Since P is a type-α N-representative, $P_{j+k} \in \operatorname{int}(P_j, P_{j+1}, P_{j+k+1})$ for all $j \geq N$. Applying Lemma 3.17 with Equation (1) on P'_j for $j \in \{i, i+1, i+2, i+k, i+k+1\}$ gives us

$$\begin{aligned} P'_i &= (1-s_1)P_{i+1} + s_1 P_{i+k+1}; & P'_{i+1} &= (1-t_1)P_{i+1} + t_1 P_{i+k+1}; \\ P'_{i+1} &= (1-s_2)P_{i+2} + s_2 P_{i+k+2}; & P'_{i+2} &= (1-t_2)P_{i+2} + t_2 P_{i+k+2}; \\ P'_{i+k} &= (1-s_3)P_{i+k+1} + s_3 P_{i+2k+1}; & P'_{i+k+1} &= (1-t_3)P_{i+k+1} + t_3 P_{i+2k+1}, \end{aligned} \tag{9}$$

where $s_1, s_2, s_3 \in (0,1)$ and $t_1, t_2, t_3 \in (1, \infty)$. In particular, this shows $P'_{i+k+1} \notin P'_i P'_{i+1}$, so the three points $P'_i, P'_{i+1}, P'_{i+k+1}$ are in general position.

To see that $(P'_i, P'_{i+1}, P'_{i+2})$ is positive, Equation (3) and (9) give us

$$\begin{aligned} \mathcal{O}(P'_i, P'_{i+1}, P'_{i+2}) &= \det(P'_{i+1} - P'_i, P'_{i+2} - P'_{i+1}) \\ &= \det((s_1 - t_1)P_{i+1} + (t_1 - s_1)P_{i+k+1}, (s_2 - t_2)P_{i+2} + (t_2 - s_2)P_{i+k+2}) \\ &= (t_1 - s_1)(t_2 - s_2)\det(P_{i+k+2} - P_{i+2}, P_{i+1} - P_{i+k+1}). \end{aligned} \tag{10}$$

Then, since $\mathcal{O}(P_{i+1}, P_{i+2}, P_{i+k+2}) > 0$ and $P_{i+k+1} \in \operatorname{int}(P_{i+1}, P_{i+2}, P_{i+k+2})$, Proposition 2.2 implies $\det(P_{i+k+2} - P_{i+2}, P_{i+1} - P_{i+k+1}) > 0$, so $\mathcal{O}(P'_i, P'_{i+1}, P'_{i+2}) > 0$.

Next, we show that $P'_{i+k} \in \operatorname{int}(P'_i, P'_{i+1}, P'_{i+k+1})$. Let $r_1 = \frac{1-s_1}{t_1 - s_1}$ and $r_2 = \frac{s_3}{t_3}$. (9) implies $r_1, r_2 \in (0,1)$ and

$$\begin{aligned} P'_{i+k} &= (1-s_3)P_{i+k+1} + s_3 P_{i+2k+1} \\ &= \frac{(1-s_3)(t_1-1)}{t_1 - s_1} P'_i + \frac{(1-s_3)(1-s_1)}{t_1 - s_1} P'_{i+1} + \frac{s_3(t_3-1)}{t_3 - s_3} P'_{i+k} + \frac{s_3(1-s_3)}{t_3 - s_3} P'_{i+k+1}. \end{aligned}$$

It follows that

$$\begin{aligned} P'_{i+k} &= \frac{t_3 - s_3}{t_3(s_3 - 1)} \left(\frac{(1-s_3)(t_1-1)}{t_1 - s_1} P'_i + \frac{(1-s_3)(1-s_1)}{t_1 - s_1} P'_{i+1} + \frac{s_3(1-s_3)}{t_3 - s_3} P'_{i+k+1} \right) \\ &= \frac{(t_3 - s_3)(1-t_1)}{t_3(t_1 - s_1)} P'_i + \frac{(t_3 - s_3)(s_1 - 1)}{t_3(t_1 - s_1)} P'_{i+1} + \frac{s_3}{t_3} P'_{i+k+1} \\ &= (1-r_2)(1-r_1)P'_i + (1-r_2)r_1 P'_{i+1} + r_2 P'_{i+k+1}. \end{aligned}$$

Observe that the coefficients $(1-r_2)(1-r_1)$, $(1-r_2)r_1$, r_2 are all in $(0,1)$ and sum up to 1, so $P'_{i+k} \in \operatorname{int}(P'_i, P'_{i+1}, P'_{i+k+1})$.

Finally, using Equation (3) and (9), we have

$$\begin{aligned}\det(P'_{i+1}-P'_i, P'_{i+k+1}-P'_{i+k}) &= \det((t_1-s_1)(P_{i+k+1}-P_{i+1}), (t_3-s_3)(P_{i+2k+1}-P_{i+k+1})) \\ &= (t_1-s_1)(t_3-s_3)\det(P_{i+k+1}-P_{i+1}, P_{i+2k+1}-P_{i+k+1}) \\ &= (t_1-s_1)(t_3-s_3)\mathcal{O}(P_{i+1}, P_{i+k+1}, P_{i+2k+1}).\end{aligned} \tag{11}$$

Proposition 3.15 implies $\mathcal{O}(P_{i+1}, P_{i+k+1}, P_{i+2k+1}) > 0$, so $\det(P'_{i+1}-P'_i, P'_{i+k+1}-P'_{i+k}) > 0$ Since $P'_i, P'_{i+1}, P'_{i+k+1}$ are in general position and $P'_{i+k} \in \operatorname{int}(P'_i, P'_{i+1}, P'_{i+k+1})$, Proposition 2.2 and Equation (11) imply $\mathcal{O}(P'_i, P'_{i+1}, P'_{i+k+1}) > 0$. We conclude that P' is a type-α N-representative. □

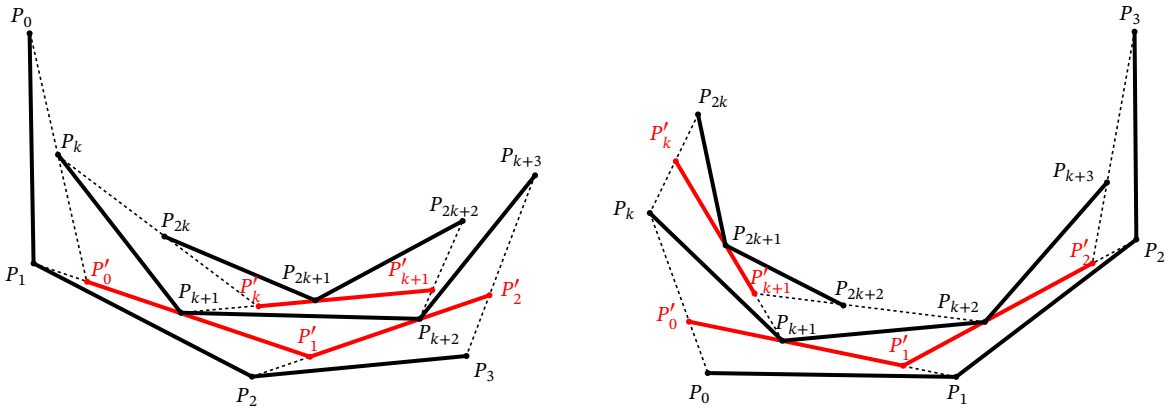

Figure 15: Left: Proposition 3.18 configuration. Right: Proposition 3.19 configuration.

Proposition 3.19. *For all $k \geq 2$ and $n \geq 2$, $T_k(\mathcal{S}^{\beta}_{k,n}) \subset \mathcal{S}^{\beta}_{k,n}$.*

Proof. The proof is analogous to the one for Proposition 3.18. Replacing α with β, we may work with the setup in the proof of Proposition 3.18. See the right side of Figure 15.

The key difference between type-α and type-β is that conditions for type-β k-spirals give us the following linear relations when we apply Lemma 3.17 with (1) on P'_j for

$j \in \{i, i+1, i+2, i+k, i+k+1\}$:

$$\begin{aligned} P'_i &= (1-t_1)P_{i+1} + t_1 P_{i+k+1}; & P'_{i+1} &= (1-s_1)P_{i+1} + s_1 P_{i+k+1}; \\ P'_{i+1} &= (1-t_2)P_{i+2} + t_2 P_{i+k+2}; & P'_{i+2} &= (1-s_2)P_{i+2} + s_2 P_{i+k+2}; \\ P'_{i+k} &= (1-t_3)P_{i+k+1} + t_3 P_{i+2k+1}; & P'_{i+k+1} &= (1-s_3)P_{i+k+1} + s_3 P_{i+2k+1}, \end{aligned} \tag{12}$$

where $s_1, s_2, s_3 \in (0,1)$ and $t_1, t_2, t_3 \in (1, \infty)$. We can see that $P'_{i+k} \notin P'_i P'_{i+1}$, so the three points P'_i, P'_{i+1}, P'_{i+k} are in general position.

A very similar computation as Equation (10) shows positivity of $(P'_i, P'_{i+1}, P'_{i+2})$, so we will omit it. Next, let $r_1 = \frac{t_1 - 1}{t_1 - s_1}$ and $r_2 = \frac{s_3}{t_3}$. Notice that $(1-r_2)(1-r_1)$, $(1-r_2)r_1$, and r_2 are all in $(0,1)$ and sum up to 1. Also, Equation (12) implies

$$P'_{i+k+1} = (1-r_2)(1-r_1)P'_i + (1-r_2)r_1 P'_{i+1} + r_2 P'_{i+k}.$$

This shows $P'_{i+k+1} \in \mathrm{int}(P'_i, P'_{i+1}, P'_{i+k})$. Finally, positivity of $(P'_i.P'_{i+1}, P'_{i+k})$ follows from a similar computation as Equation (11), $P'_{i+k+1} \in \mathrm{int}(P'_i, P'_{i+1}, P'_{i+k})$, the points P'_i, P'_{i+1}, P'_{i+k} are in general position, and Proposition 2.2. □

3.4 Invariance of Backward Orbit

In this section, we complete the proof of Theorem 1.1 by showing that $\mathcal{S}^{\alpha}_{k,n}$ and $\mathcal{S}^{\beta}_{k,n}$ are T_k^{-1}-invariant. One can derive a formula for T_k^{-1} from Equation (1). Given any k-nice twisted n-gon P', $P = T_k^{-1}(P')$ is given by

$$P_i = P'_{i-k-1}P'_{i-k} \cap P'_{i-1}P'_i. \tag{13}$$

Proposition 3.8 implies T_k^{-1} is well-defined on $\mathcal{S}^{\alpha}_{k,n}$ and $\mathcal{S}^{\beta}_{k,n}$. In general, T_k^{-1} needs not preserve k-niceness of twisted polygons.

Proposition 3.20. *For all $k \geq 2$ and $n \geq 2$, $T_k^{-1}(S^{\alpha}_{k,n}) \subset S^{\alpha}_{k,n}$.*

Proof. Given P' a type-α N-representative, we will show that $P = T_k^{-1}(P')$ is a type-α $(N+k+1)$-representative by proving that for all $i \geq N+k+1$, (P_i, P_{i+1}, P_{i+2}) is positive,

$(P_i, P_{i+1}, P_{i+k+1})$ is positive, the four points $P_i, P_{i+1}, P_{i+k}, P_{i+k+1}$ are in general position, and $P_{i+k} \in \operatorname{int}(P_i, P_{i+1}, P_{i+k+1})$. See the left side of Figure 16 for configurations of relevant vertices of P' and P.

Let $i \geq N + k + 1$ be fixed. Since P' is a type-α N-representative, we must have $P'_{j+k} \in \operatorname{int}(P'_j, P'_{j+1}, P'_{j+k+1})$ for all $j \geq N$. Applying Lemma 3.17 with Equation (13) on P_j for $j \in \{i, i+1, i+2, i+k, i+k+1\}$ gives us

$$\begin{aligned}
&P_i = (1-s_1)P'_{i-k} + s_1 P'_{i-k-1}; && P_i = (1-t_1)P'_i + t_1 P'_{i-1};\\
&P_{i+1} = (1-s_2)P'_{i-k+1} + s_2 P'_{i-k}; && P_{i+1} = (1-t_2)P'_{i+1} + t_3 P'_i;\\
&P_{i+2} = (1-s_3)P'_{i-k+2} + s_3 P'_{i-k+1}; && P_{i+k} = (1-s_4)P'_i + s_4 P'_{i-1};\\
&P_{i+k+1} = (1-s_5)P'_{i+1} + s_5 P'_i,
\end{aligned} \tag{14}$$

where $s_1, s_2, s_3, s_4, s_5 \in (0,1)$ and $t_1, t_2 \in (1, \infty)$.

We first show that $(P_i, P_{i+1}, P_{i+k+1})$ is positive. From Equation (14) we have

$$\mathcal{O}(P_i, P_{i+1}, P_{i+k+1}) = (t_1 t_2 (1-s_5) - t_1(1-t_2)s_5)\mathcal{O}(P'_{i-1}, P'_i, P'_{i+1}).$$

It follows that $\mathcal{O}(P_i, P_{i+1}, P_{i+k+1}) > 0$, so $(P_i, P_{i+1}, P_{i+k+1})$ is positive.

Next, we show that $P_{i+k} \in \operatorname{int}(P_i, P_{i+1}, P_{i+k+1})$. Let $r_1 = \frac{t_2 - 1}{t_2 - s_5}$ and $r_2 = \frac{s_4}{t_1}$. Equation (14) implies $r_1, r_2 \in (0,1)$ and

$$P_{i+k} = (1-r_2)(1-r_1)P_{i+1} + (1-r_2)r_1 P_{i+k+1} + r_2 P_i.$$

Observe that the coefficients $(1-r_2)(1-r_1)$, $(1-r_2)r_1$, and r_2 are all in $(0,1)$ and sum up to 1, so $P_{i+k} \in \operatorname{int}(P_i, P_{i+1}, P_{i+k+1})$.

Finally, we check (P_i, P_{i+1}, P_{i+2}) is positive. We aim to invoke Lemma 3.14 with the following choices of vertices:

$$O = P_{i+1};\ \ A = P_i;\ \ B = P_{i+k+1};\ \ C = P_{i+2};\ \ D = P'_{i-k+1}. \tag{15}$$

Positivity of (A, O, B) is a direct consequence of the above argument. Positivity of (B, O, C) follows from positivity of $(P_{i+1}, P_{i+2}, P_{i+k+2})$, $P_{i+k+1} \in \operatorname{int}(P_{i+1}, P_{i+2}, P_{i+k+2})$, and Proposition

2.2. Next, observe that

$$\begin{aligned}
\mathcal{O}(A,O,D) &= s_1 s_2 \mathcal{O}(P'_{i-k-1}, P'_{i-k}, P'_{i-k+1});\\
\mathcal{O}(C,O,D) &= (1-s_3) s_2 \mathcal{O}(P'_{i-k}, P'_{i-k+1}, P'_{i-k+2});\\
\mathcal{O}(B,O,D) &= s_2(1-s_5)\mathcal{O}(P'_{i-k}, P'_{i-k+1}, P'_{i+1}) + s_2 s_5 \mathcal{O}(P'_{i-k}, P'_{i-k+1}, P'_i);
\end{aligned} \tag{16}$$

Then, positivity of (A,O,D) and (C,O,D) follows from positivity of $(P'_{i-k-1}, P'_{i-k}, P'_{i-k+1})$ and $(P'_{i-k}, P'_{i-k+1}, P'_{i-k+2})$. To see that (B,O,D) is positive, apply Proposition 2.2 on $(P'_{i-k}, P'_{i-k+1}, P'_{i+1})$ positive and $P'_i \in \mathrm{int}(P'_{i-k}, P'_{i-k+1}, P'_{i+1})$ to get $(P'_{i-k}, P'_{i-k+1}, P'_i)$ positive. The backward direction of Lemma 3.14 then implies (P_i, P_{i+1}, P_{i+2}) is positive. We conclude that P is a type-α $(N+k+1)$-representative. □

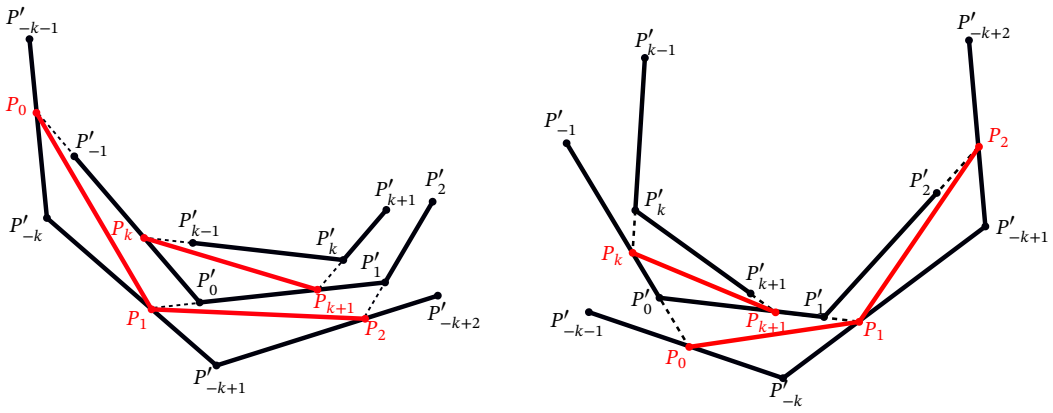

Figure 16: Left: Proposition 3.20 configuration. Right: Proposition 3.21 configuration.

Proposition 3.21. *For all $k \geq 2$ and $n \geq 2$, $T_k^{-1}(S^{\beta}_{k,n}) \subset S^{\beta}_{k,n}$.*

Proof. The proof is similar to that of Lemma 3.20 (See right side of Figure 16). We will point out some key differences. Replacing α with β, we may work with the setup in the proof of Proposition 3.20. Applying Lemma 3.17 with (13) on P_j for $j \in \{i, i+1, i+2, i+k, i+k+1\}$

gives us

$$\begin{aligned} P_i &= (1-s_1)P'_{i-k} + s_1 P'_{i-k-1}; & P_i &= (1-t_1)P'_{i-1} + t_1 P'_i; \\ P_{i+1} &= (1-s_2)P'_{i-k+1} + s_2 P'_{i-k}; & P_{i+1} &= (1-t_2)P'_i + t_3 P'_{i+1}; \\ P_{i+2} &= (1-s_3)P'_{i-k+2} + s_3 P'_{i-k+1}; & P_{i+k} &= (1-s_4)P'_{i-1} + s_4 P'_i; \\ P_{i+k+1} &= (1-s_5)P'_i + s_5 P'_{i+1}, \end{aligned} \tag{17}$$

where $s_1, s_2, s_3, s_4, s_5 \in (0,1)$ and $t_1, t_2 \in (1,\infty)$. Positivity of (P_i, P_{i+1}, P_{i+k}) follows from a similar computation as in (3.4). Next, let $r_1 = \frac{1-s_4}{t_1-s_4}$ and $r_2 = \frac{s_5}{t_2}$. Equation (17) implies

$$P_{i+k+1} = (1-r_2)(1-r_1)P_{i+k} + (1-r_2)r_1 P_i + r_2 P_{i+1}.$$

Observe that the coefficients $(1-r_2)(1-r_1)$, $(1-r_2)r_1$, and r_2 are all in $(0,1)$ and sum up to 1, so $P_{i+k+1} \in \operatorname{int}(P_i, P_{i+1}, P_{i+k})$.

Finally, assign O, A, B, C, D to be the same vertices as in (15). Positivity of (A,O,B), (B,O,C), (C,O,D), (A,O,D), and (B,O,D) follows from a very similar proof as that of Proposition 3.20, with (16) replaced by

$$\begin{aligned} \mathcal{O}(A,O,D) &= s_1 s_2 \mathcal{O}(P'_{i-k-1}, P'_{i-k}, P'_{i-k+1}); \\ \mathcal{O}(C,O,D) &= (1-s_3)s_2 \mathcal{O}(P'_{i-k}, P'_{i-k+1}, P'_{i-k+2}); \\ \mathcal{O}(B,O,D) &= s_2(1-s_5)\mathcal{O}(P'_{i-k}, P'_{i-k+1}, P'_i) + s_2 s_5 \mathcal{O}(P'_{i-k}, P'_{i-k+1}, P'_{i+1}). \end{aligned}$$

The backward direction of Proposition 3.14 then implies (P_i, P_{i+1}, P_{i+2}) is positive. □

We conclude this section by stating that Proposition 3.18, 3.19, 3.20, 3.21 together prove Theorem 1.1.

4 Coordinate Representation of 3-Spirals

4.1 The Tic-Tac-Toe Grids

Recall the intervals $I = (-\infty, 0)$, $J = (0,1)$, $K = (1,\infty)$ from §1.3. One can partition $\mathbb{R}^2$ into a 3×3 grid. See Figure 5. We make the following definition:

Definition 4.1. For $n \geq 2$, let $S_n(I,J)$ be the subset of $\mathcal{P}_n$ that satisfies the following: given $[P] \in S_n(I,J)$, for all $i \in \{0,\dots,n-1\}$, $(x_{2i}, x_{2i+1}) \in I \times J$. We similarly define $S_n(K,J)$, $S_n(J,I)$, and $S_n(J,K)$.

The following symmetries of the four grids follow directly from Definition 4.1.

Proposition 4.2. *For $i \in \mathbb{Z}$, define the map $\sigma_i : \mathbb{Z} \to \mathbb{Z}$ by $\sigma_i(x) = x + i$. Define the map $\iota : \mathbb{Z} \to \mathbb{Z}$ by $\iota(x) = -x$. Given $[P] \in \mathcal{P}_n$, the following are true:*

- *If $[P] \in S_n(I,J)$, then $[P \circ \sigma_i] \in S_n(I,J)$ for all $i \in \mathbb{Z}$. This also holds for $S_n(K,J)$, $S_n(J,I)$, and $S_n(J,K)$.*
- *$[P] \in S_n(I,J)$ if and only if $[P \circ \iota] \in S_n(J,I)$.*
- *$[P] \in S_n(K,J)$ if and only if $[P \circ \iota] \in S_n(J,K)$.*

To understand the geometry implied by the corner invariants, we need to examine what happens when the corner invariants take value from $0, 1, \infty$.

Proposition 4.3. *For all $[P] \in \mathcal{P}_n$ with corner invariants $x_j = x_j(P)$ and $i \in \mathbb{Z}$, we have the following correspondence between the position of P_{i+2} and the values of x_{2i} and x_{2i+1}:*

Configuration	*Coordinates*	*Configuration*	*Coordinates*
$P_{i+2} \in P_{i+1}P_i$	$x_{2i} = 0$	$P_{i+2} \in P_{i-1}P_{i+1}$	$x_{2i+1} = 0$
$P_{i+2} \in P_{i+1}P_{i-2}$	$x_{2i} = 1$	$P_{i+2} \in P_{i-1}P_{i-2}$	$x_{2i+1} = 1$
$P_{i+2} \in P_{i+1}P_{i-1}$	$x_{2i} = \infty$	$P_{i+2} \in P_{i-1}P_i$	$x_{2i+1} = \infty$

Proof. Consider the following lines:

$$l_1 = P_{i+1}P_{i-2}; \quad l_2 = P_{i+1}P_{i-1}; \quad l_3 = P_{i+1}P_i; \quad l_4 = P_{i+1}P_{i+2};$$
$$m_1 = P_{i-1}P_{i+2}; \quad m_2 = P_{i-1}P_{i+1}; \quad m_3 = P_{i-1}P_i; \quad m_4 = P_{i-1}P_{i-2}.$$

See Figure 17 for a visualization of the configurations of points and lines. Equation (8) implies $x_{2i} = \chi(l_1, l_2, l_3, l_4)$ and $x_{2i+1} = \chi(m_1, m_2, m_3, m_4)$. This yields

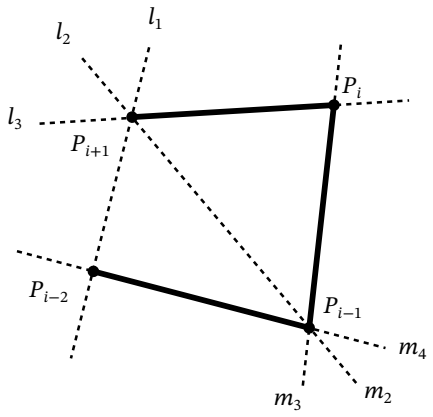

Figure 17: Configurations of points and lines in the proof of Proposition 4.3.

Configuration	Lines	Coordinates	Configuration	Lines	Coordinates
$P_{i+2} \in P_{i+1}P_i$	$l_4 = l_3$	$x_{2i} = 0$	$P_{i+2} \in P_{i-1}P_{i+1}$	$m_1 = m_2$	$x_{2i+1} = 0$
$P_{i+2} \in P_{i+1}P_{i-2}$	$l_4 = l_1$	$x_{2i} = 1$	$P_{i+2} \in P_{i-1}P_{i-2}$	$m_1 = m_4$	$x_{2i+1} = 1$
$P_{i+2} \in P_{i+1}P_{i-1}$	$l_4 = l_2$	$x_{2i} = \infty$	$P_{i+2} \in P_{i-1}P_i$	$m_1 = m_3$	$x_{2i+1} = \infty$

which is precisely the relationship described in the proposition. □

Remark 4.4. Proposition 4.3 also gives us a way to determine the position of P_{i+2} when neither x_{2i} nor x_{2i+1} takes value in $0, 1, \infty$. Suppose the four points $P_{i-2}, P_{i-1}, P_i, P_{i+1}$ are in general position. For $i, j, k \in \{1, 2, 3\}$ distinct, we define $U_{i,j}$ to be the connected component of $\mathbb{RP}^2 - (l_i \cup l_j)$ that does not intersect l_k. For $i, j, k \in \{2, 3, 4\}$ distinct, we define $V_{i,j}$ to be the connected component of $\mathbb{RP}^2 - (m_i \cup m_j)$ that does not intersect m_k. See Figure 18 for a visualization of the $U_{i,j}$'s and $V_{i,j}$'s using the point configurations given in Figure 17. By Proposition 4.3 and continuity of χ, we have the following:

Configuration	Coordinates	Configuration	Coordinates
$P_{i+2} \in U_{2,3}$	$x_{2i} = I$	$P_{i+2} \in V_{2,3}$	$x_{2i+1} = I$
$P_{i+2} \in U_{1,3}$	$x_{2i} = J$	$P_{i+2} \in V_{2,4}$	$x_{2i+1} = J$
$P_{i+2} \in U_{1,2}$	$x_{2i} = K$	$P_{i+2} \in V_{3,4}$	$x_{2i+1} = K$

Corollary 4.5. *Given $[P] \in \mathcal{P}_n$ with corner invariants $x_j = x_j(P)$, if $x_j \notin \{0, 1, \infty\}$ for all j, then P is 3-nice. Moreover, every four consecutive points of P are in general position.*

Proof. Using Proposition 4.3 we may check that

Collinearity	Coordinates	Collinearity	Coordinates
$P_{i-2}, P_{i-1}, P_{i+1}$	$x_{2i-1} = \infty$	P_{i-1}, P_i, P_{i+2}	$x_{2i+1} = \infty$
$P_{i-2}, P_{i-1}, P_{i+2}$	$x_{2i+1} = 1$	$P_{i-1}, P_{i+1}, P_{i+2}$	$x_{2i+1} = 0$
$P_{i-2}, P_{i+1}, P_{i+2}$	$x_{2i} = 1$	P_i, P_{i+1}, P_{i+2}	$x_{2i} = 0$
P_{i-1}, P_i, P_{i+1}	$x_{2i-2} = 0$		

All seven cases contradict the assumption in the corollary. Therefore, the four points $P_{i-2}, P_{i-1}, P_{i+1}, P_{i+2}$ are in general position, and the four consecutive points $P_{i-1}, P_i, P_{i+1}, P_{i+2}$ are in general position for all $i \in \mathbb{Z}$. This shows P is 3-nice, and every four consecutive points of P are in general position. □

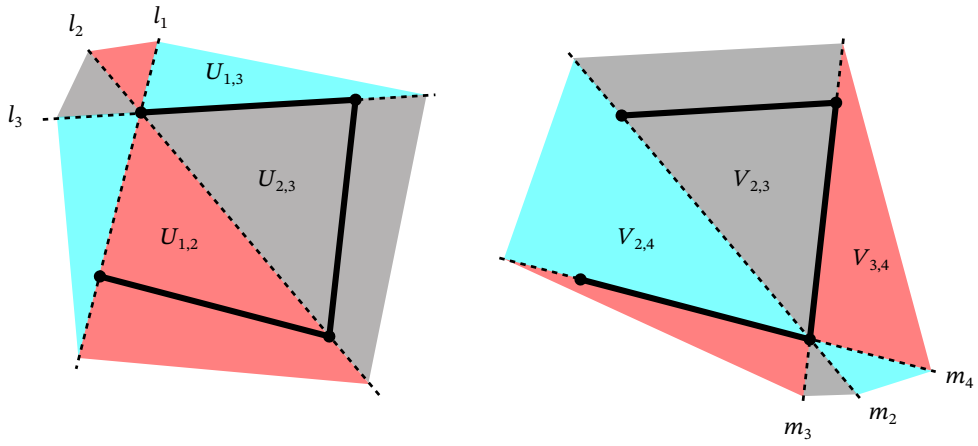

Figure 18: The connected components $U_{i,j}$'s and $V_{i,j}$'s in Remark 4.4. The corner invariants value in I if P_{i+2} lies in the black-shaded region, J if P_{i+2} lies in the red-shaded region, and K if P_{i+2} lies in the cyan-shaded region.

Our goal of this section is to prove the following correspondence theorem:

Theorem 4.6. *For all $n \geq 2$, $\mathcal{S}^{\alpha}_{3,n} = S_n(J,I)$, $\mathcal{S}^{\beta}_{3,n} = S_n(K,J)$.*

This theorem immediately produces the following important corollary.

Corollary 4.7. *For all $n \geq 2$, the four cells $S_n(I,J)$, $S_n(K,J)$, $S_n(J,I)$, $S_n(J,K)$ are both forward and backward invariant under T_3.*

Proof. The case $S_n(J,I)$ and $S_n(K,J)$ follows immediately from Theorem 1.1 and 4.6. We will prove the case $S_n(I,J)$. The case $S_n(J,K)$ is completely analogous, so we will omit.

Fix $[P] \in S_n(I,J)$. Recall the maps σ_i and ι from Proposition 4.2. Equation (1) implies $T_3(P \circ \iota) = T_3(P) \circ \iota \circ \sigma_4$. Then, Proposition 4.2 implies $[P \circ \iota] \in S_n(J,I)$, so $[T_3(P \circ \iota)] \in S_n(J,I)$. Finally, observe that

$$T_3(P) = (T_3(P) \circ \iota \circ \sigma_4) \circ (\sigma_{-4} \circ \iota) = T_3(P \circ \iota) \circ (\sigma_{-4} \circ \iota).$$

It follows that $[T_3(P)] \in S_n(I,J)$. We omit the proof of $[T_3^{-1}(P)] \in S_n(I,J)$. □

4.2 The Correspondence of $\mathcal{S}^{\alpha}_{3,n}$ and $S_n(J,I)$

Here we show that $\mathcal{S}^{\alpha}_{3,n}$ is equivalent to $S_n(J,I)$. We will first show that the corner invariants of a 0-representative P of some $[P] \in \mathcal{S}^{\alpha}_{3,n}$ satisfies $S_n(J,I)$. Then, we will show that we can find type-α N-representatives for all $N \in \mathbb{Z}$ given any $[P] \in S_n(J,I)$.

Lemma 4.8. *If P is an N-representative of $[P] \in \mathcal{S}^{\alpha}_{3,n}$, then $P_{i+2} \in \operatorname{int}(P_{i-1}, P_i, P_{i+1})$ for all $i > N+1$.*

Proof. Since (P_{i-1}, P_i, P_{i+1}) is positive, we may normalize with $\mathrm{Aff}_2^+(\mathbb{R})$ so that $P_{i-1} = (-1,0)$, $P_i = (0,0)$, and $P_{i+1} = (0,1)$. Let $P_{i+2} = (x,y)$. It suffices to show that $x < 0$, $y > 0$, and $y - x < 1$. We get $x < 0$ from positivity of (P_i, P_{i+1}, P_{i+2}), and we get $y > 0$ from positivity of (P_{i-1}, P_i, P_{i+2}). Finally, since $(P_{i-2}, P_{i-1}, P_{i+2})$ is positive and $P_{i+1} \in \operatorname{int}(P_{i-2}, P_{i-1}, P_{i+2})$, Proposition 2.2 implies $(P_{i+1}, P_{i-1}, P_{i+2})$ is positive, which gives us $y - x < 1$ as desired. □

Proposition 4.9. *For all $n \geq 2$, $\mathcal{S}^{\alpha}_{3,n} \subset S_n(J,I)$.*

Proof. Fix $i \in \mathbb{Z}$. Let P be an $(i-3)$-representative of $[P] \in \mathcal{S}^{\alpha}_{3,n}$ with corner invariants $x_j = x_j(P)$. Normalize with $\mathrm{Aff}^+_2(\mathbb{R})$ so that $P_{i-1} = (-1,0)$, $P_i = (0,0)$, and $P_{i+1} = (0,1)$. Let $s_{a,b}$ denote the slope of the line $P_{i+a}P_{i+b}$. See Figure 19 for the configuration of points.

We want to show that $(x_{2i}, x_{2i+1}) \in I \times J$. By Lemma 4.8, $P_{i+1} \in \mathrm{int}(P_{i-2}, P_{i-1}, P_i)$. This implies $s_{1,-2} > s_{-1,-2} > 1$. On the other hand, since $P_{i+1} \in \mathrm{int}(P_{i-2}, P_{i-1}, P_{i+2})$, we have $s_{1,2} > s_{1,-2} > 1$, and $s_{-1,2} \in (0,1)$. This gives us

$$x_{2i} = \frac{(s_{1,-2} - s_{1,-1})(s_{1,0} - s_{1,2})}{(s_{1,-2} - s_{1,0})(s_{1,-1} - s_{1,2})} = \frac{s_{1,-2} - 1}{s_{1,2} - 1} \in J \qquad \text{and}$$
$$x_{2i+1} = \frac{(s_{-1,2} - s_{-1,1})(s_{-1,0} - s_{-1,-2})}{(s_{-1,2} - s_{-1,0})(s_{-1,1} - s_{-1,-2})} = \frac{s_{-1,-2}(s_{-1,2} - 1)}{s_{-1,2}(s_{-1,-2} - 1)} \in I.$$

This concludes the proof. □

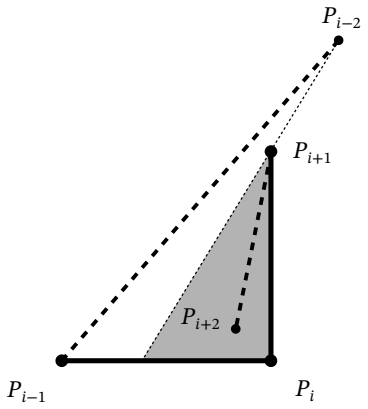

Figure 19: Configuration of Proposition 4.9 and 4.10.

Proposition 4.10. *For all $n \geq 2$, $\mathcal{S}^{\alpha}_{3,n} = S_n(I,J)$.*

Proof. Proposition 4.9 implies we only need to show $\mathcal{S}^{\alpha}_{3,n} \supset S_n(I,J)$. Given $[P] \in S_n(I,J)$, let P be a representative that satisfies $P_{-1} = (1,4)$, $P_0 = (-1,0)$, $P_1 = (0,0)$, $P_2 = (0,1)$. Say that P satisfies condition $(*)_i$ if the three triangles (P_{i-1}, P_i, P_{i+1}), (P_i, P_{i+1}, P_{i+2}), (P_{i-1}, P_i, P_{i+2}) are all positive, $P_{i+2} \in \mathrm{int}(P_{i-1}, P_i, P_{i+1})$, and $P_{i+2} \in \mathrm{int}(P_{i-2}, P_{i-1}, P_{i+1})$.

We show that for all $i > 0$, if P satisfies $(*)_{i-1}$, then P satisfies $(*)_i$. Since (P_{i-1}, P_i, P_{i+1}) is positive, we can normalize with $\mathrm{Aff}^+_2(\mathbb{R})$ so that $P_{i-1} = (-1,0)$, $P_i = (0,0)$, and $P_{i+1} =$

$(0,1)$. Let $s_{a,b}$ denote the slope of $P_{i+a}P_{i+b}$. Since $P_{i+1} \in \operatorname{int}(P_{i-2}, P_{i-1}, P_i)$, we know that $s_{1,-2} > s_{-1,-2} > 1$. Then, $x_{2i} \in J$ implies $0 < \frac{s_{1,-2}-1}{s_{1,2}-1} < 1$. This gives us $s_{1,2} > s_{1,-2} > 1$. On the other hand, $x_{2i+1} \in I$ implies $\frac{s_{-1,-2}(s_{-1,2}-1)}{s_{-1,2}(s_{-1,-2}-1)} < 0$. Since $s_{-1,-2} > 1$, this is equivalent to $1 - \frac{1}{s_{-1,2}} < 0$, which implies $s_{-1,2} \in (0,1)$. Thus, the two lines $P_{i-1}P_{i+2}$ and $P_{i+1}P_{i+2}$ must meet in the shaded triangle in Figure 19, which implies (P_i, P_{i+1}, P_{i+2}), (P_{i-1}, P_i, P_{i+2}) are positive, $P_{i+2} \in \operatorname{int}(P_{i-1}, P_i, P_{i+1})$, and $P_{i+2} \in \operatorname{int}(P_{i-2}, P_{i-1}, P_{i+1})$, so P satisfies $(*)_i$. Finally, since P clearly satisfies $(*)_0$, by induction P satisfies $(*)_i$ for all $i \geq 0$, so P is a type-α 0-representative of a 3-spiral. We conclude that $[P] \in \mathcal{S}^{\alpha}_{3,n}$. □

4.3 The Correspondence of $\mathcal{S}^{\beta}_{3,n}$ and $S_n(K,J)$

Here we show that $\mathcal{S}^{\beta}_{3,n}$ is equivalent to $S_n(K,J)$. The ideas behind the proofs are essentially the same as the ones in §4.2. We will focus on explaining how to modify the details of the proofs in §4.2 for type-β 3-spirals and $S_n(K,J)$.

Lemma 4.11. *If P is an N-representative of $[P] \in \mathcal{S}^{\beta}_{3,n}$, then the quadrilateral joined by vertices $(P_i, P_{i+1}, P_{i+2}, P_{i+3})$ is convex for all $i > N$.*

Proof. Normalize with $\operatorname{Aff}_2^+(\mathbb{R})$ so that $P_i = (-1,0)$, $P_{i+1} = (0,0)$, $P_{i+2} = (0,1)$, and $P_{i+3} = (x,y)$. Positivity of $(P_{i+1}, P_{i+2}, P_{i+3})$ and (P_i, P_{i+1}, P_{i+3}) implies $x < 0$ and $y > 0$. Positivity of (P_{i-1}, P_i, P_{i+2}), $P_{i+3} \in \operatorname{int}(P_{i-1}, P_i, P_{i+2})$, and Proposition 2.2 shows $y - x > 1$. □

Proposition 4.12. *For all $n \geq 2$, $\mathcal{S}^{\beta}_{3,n} \subset S_n(K,J)$.*

Proof. Let P be a (-3)-representative of $[P] \in \mathcal{S}^{\beta}_{3,n}$ with corner invariants $x_j = x_j(P)$. Lemma 4.11 implies the quadrilateral $(P_{i-2}, P_{i-1}, P_i, P_{i+1})$ is convex. Next, since P is a type-β (-3)-representative, $P_i \in \operatorname{int}(P_{i-2}, P_{i-1}, P_{i+1})$ for all $i \geq 0$ (See Figure 20). Referring back to Remark 4.4, convexity of $(P_{i-2}, P_{i-1}, P_i, P_{i+1})$ implies P_iP_{i+1} doesn't go through $P_{i-2}, P_{i-1}, P_{i+1}$, so $(x_{2i}, x_{2i+1}) \in K \times J$ whenever $P_{i+2} \in \operatorname{int}(P_{i-2}, P_{i-1}, P_{i+1})$. □

Lemma 4.13. *Given a 3-nice sequence $P : \mathbb{Z} \to \mathbb{RP}^2$ and an integer $i \in \mathbb{Z}$, let $x_{2i} = x_{2i}(P)$ and $x_{2i+1} = x_{2i+1}(P)$ be the corner invariants of P. If the following conditions are true:*

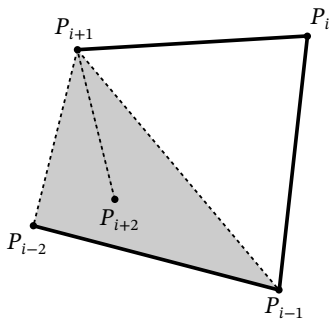

Figure 20: Configuration of Proposition 4.12 and Lemma 4.13.

- (P_{i-2}, P_{i-1}, P_i) *and* (P_{i-1}, P_i, P_{i+1}) *are both positive;*
- *The quadrilateral* $(P_{i-2}, P_{i-1}, P_i, P_{i+1})$ *is convex;*
- $(x_{2i}, x_{2i+1}) \in K \times J$.

Then, the following hold:

- $P_{i+2} \in \operatorname{int}(P_{i-2}, P_{i-1}, P_{i+1})$*;*
- *The quadrilateral* $(P_{i-1}, P_i, P_{i+1}, P_{i+2})$ *is convex;*
- (P_i, P_{i+1}, P_{i+2}) *and* (P_{i-1}, P_i, P_{i+2}) *are both positive.*

Proof. Recall that from the proof of Proposition 4.12, we claimed that if the quadrilateral $(P_{i-2}, P_{i-1}, P_i, P_{i+1})$ is convex, then the line P_iP_{i+1} doesn't go through $(P_{i-2}, P_{i-1}, P_{i+1})$. Since $(x_{2i}, x_{2i+1}) \in K \times J$, Remark 4.4 implies $P_{i+2} \in \operatorname{int}(P_{i-2}, P_{i-1}, P_{i+1})$, in which case all conclusions of this lemma will hold. See Figure 20 for a visualization of the five points. □

Proposition 4.14. $\mathcal{S}^{\beta}_{3,n} = S_n(K, J)$.

Proof. Proposition 4.12 gives us $\mathcal{S}^{\beta}_{3,n} \subset S_n(K, J)$, so we show the other containment. Given $[P] \in S_n(K, J)$, we can find a representative P that satisfies $P_N = (0, 0)$, $P_{N+1} = (1, 0)$, $P_{N+2} = (1, 1)$, $P_{N+3} = (0, 1)$. Corollary 4.5 shows that P is 3-nice. To see that (P_i, P_{i+1}, P_{i+2}), (P_i, P_{i+1}, P_{i+3}) are positive, and $P_{i+4} \in \operatorname{int}(P_i, P_{i+1}, P_{i+3})$, we may inductively apply Lemma 4.13. This implies $[P] \in \mathcal{S}^{\beta}_{3,n}$. □

5 A Birational Formula for T_3

Given two spaces X and Y, a *rational map* $f : X \dashrightarrow Y$ is an equivalence class of maps $f_U : U \to Y$ where U is a dense open in X, and the equivalence relation is given by $f_U \sim f_V$ if they restrict to the same map on $U \cap V$. A map $f : X \dashrightarrow Y$ is *birational* if there exists a rational map $g : Y \dashrightarrow X$ such that $g \circ f$ restricts to the identity on a dense open of X and $f \circ g$ restricts to an identity on a dense open of Y.

In this section, we show that $T_3 : \mathcal{P}_n \dashrightarrow \mathcal{P}_n$ is a birational map by finding an explicit formula using the corner invariants.

5.1 The Formula

Let P be a twisted n-gon, and $P' = T_3(P)$. In this section, we use a different labeling convention:

$$P'_i = P_{i-2}P_{i+1} \cap P_{i-1}P_{i+2}. \tag{18}$$

We let $x_j = x_j(P)$ and $x'_j = x_j(P')$ denote the corner invariants of P and P' respectively. Our goal is to show that T_3 is a birational map over the corner invariants. I discovered it using computer algebra and the reconstruction formula in [Sch08, Equation (19)].

Proposition 5.1. *Given* $[P] \in \mathcal{P}_{3,n}$*, the following formula holds* (*indices taken modulo* $2n$)*:*

$$\begin{cases} x'_{2i} = x_{2i-2} \cdot \dfrac{(x_{2i-4} + x_{2i-1} - 1)}{x_{2i-2}x_{2i-1} - (1 - x_{2i+1})(1 - x_{2i-4})}; \\ x'_{2i+1} = x_{2i+3} \cdot \dfrac{(x_{2i+2} + x_{2i+5} - 1)}{x_{2i+2}x_{2i+3} - (1 - x_{2i+5})(1 - x_{2i})}. \end{cases} \tag{19}$$

One can verify Equation (19) with the following procedure: Given the corner invariants of $[P]$, use the reconstruction formula from [Sch08, Equation (19)] to obtain a representative P. Apply T_3 on P as in Equation (18) to get $P' = T_3(P)$. Then, compute the corner invariants of P'. We present a geometric proof of Equation (19) using cross-ratio identities. We start with the following lemma, which is a classical observation in projective geometry called "quadrangular sets."

Lemma 5.2. *Let Q_1, Q_2, Q_3, Q_4 be four points in general position, and let ω be a line that contains none of the four points. For all $i \neq j$, let $l_{ij} = Q_iQ_j$ and $S_{ij} = \omega \cap l_{ij}$ Then,*

$$\chi(S_{12}, S_{13}, S_{14}, S_{24}) = \chi(S_{23}, S_{13}, S_{34}, S_{24}).$$

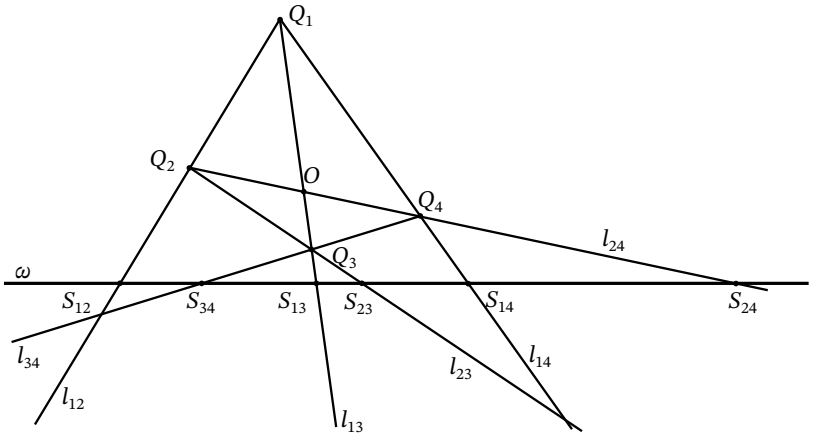

Figure 21: Point configurations of Lemma 5.2

Proof. Let $O = l_{13} \cap l_{24}$. See Figure 21 for an example of the point configurations. Applying Equation (6) on $(l_{12}, l_{13}, l_{14}, Q_1D)$ with respect to ω and Q_2Q_4 gives us

$$\chi(S_{12}, S_{13}, S_{14}, S_{24}) \overset{\omega}{=} \chi(l_{12}, l_{13}, l_{14}, Q_1D) \overset{l_{24}}{=} \chi(Q_2, O, Q_4, S_{24}).$$

Next, applying Equation (6) twice on $(l_{23}, l_{13}, l_{34}, Q_3D)$ with respect to l_{24} and ω gives us

$$\chi(Q_2, O, Q_4, S_{24}) \overset{l_{24}}{=} \chi(l_{23}, l_{13}, l_{34}, Q_3D) \overset{\omega}{=} \chi(S_{23}, S_{13}, S_{34}, S_{24}).$$

Combining the above two equations completes the proof. □

Proof of Proposition 5.1. From the symmetry of Equation (19), it suffices to prove the formula for x_0'. That is,

$$x_0' = \frac{x_{-2}(x_{-4} + x_{-1} - 1)}{x_{-2}x_{-1} - (1 - x_{-4})(1 - x_1)}. \tag{20}$$

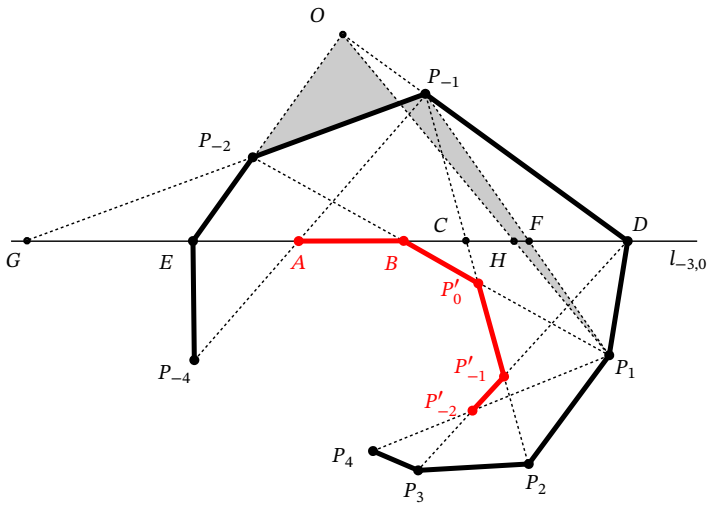

Figure 22: Visualization of Points Assigned in Equation (21). The thick black line segments are edges connecting vertices of P, and the thick red line segments are edges connecting vertices of P'.

Let $l_{i,j} = P_iP_j$ and $O = l_{-3,-2} \cap l_{-1,0}$. We label points as follows:

$$\begin{aligned} A &= P'_{-2}; & C &= l_{-3,0} \cap l_{-2,1}; & E &= P_{-3}; & G &= l_{-3,0} \cap l_{-2,-1}; \\ B &= P'_{-1}; & D &= P_0; & F &= l_{-3,0} \cap l_{-1,1}; & H &= l_{-3,0} \cap OP_1. \end{aligned} \tag{21}$$

Since $[P] \in \mathcal{P}_{3,n}$, every five consecutive points of $[P]$ are in general position. This ensures that point O and the points in Equation (21) are all distinct. See Figure 22 for a visualization of the assignment of labels to these points.

It follows from Equation (7) that $x'_0 = \chi(A, B, C, D)$. Using Equation (8), we have

$$\begin{aligned} x_{-4} &= \chi(l_{-1,-4}, l_{-1,-3}, l_{-1,-2}, l_{-1,0}) \overset{l_{-3,0}}{=} \chi(A, E, G, D); \\ x_{-2} &= \chi(l_{0,-3}, l_{0,-2}, l_{0,-1}, l_{0,1}) \overset{l_{-3,0}}{=} \chi(E, B, H, D); \\ x_{-1} &= \chi(l_{-2,1}, l_{-2,0}, l_{-2,-1}, l_{-2,-3}) \overset{l_{-3,0}}{=} \chi(B, D, G, E); \\ x_1 &= \chi(l_{-1,2}, l_{-1,1}, l_{-1,0}, l_{-1,-2}) \overset{l_{-3,0}}{=} \chi(C, F, D, G). \end{aligned} \tag{22}$$

We may further invoke Lemma 5.2 with $Q_1 = P_{-2}$, $Q_2 = O$, $Q_3 = P_1$, $Q_4 = P_{-1}$, and

$\omega = l_{-3,0}$. This gives us

$$x_{-2} = \chi(E, B, H, D) = \chi(G, B, F, D). \tag{23}$$

The rest of the proof is just algebraic verification. Normalize with a projective transformation so that $l_{-3,0}$ is the x-axis of $\mathbb{A}^2$. Let a, b, c, d, e, f, g, h be coordinates of A, B, C, D, E, F, G, H respectively. Plugging (22) and (23) into the numerator of (20) gives us

$$\begin{aligned} x_{-2}(x_{-4} + x_{-1} - 1) &= \chi(G, B, F, D)\,(\chi(A, E, G, D) + \chi(B, D, G, E) - 1) \\ &= \frac{(g-b)(f-d)}{(g-f)(b-d)}\left(\frac{(a-e)(g-d)}{(a-g)(e-d)} + \frac{(b-e)(g-d)}{(b-g)(e-d)}\right) \\ &= \frac{(a-b)(g-d)(e-g)(d-f)}{(a-g)(b-d)(e-d)(g-f)}. \end{aligned}$$

The denominator can be computed similarly. We skip the computation and list the results:

$$x_{-2}x_{-1} - (1 - x_{-4})(1 - x_1) = \frac{(a-c)(g-d)(d-f)(e-g)}{(a-g)(c-d)(d-e)(f-g)}.$$

Combining the above two equations gives us

$$\frac{x_{-2}(x_{-4} + x_{-1} - 1)}{x_{-2}x_{-1} - (1 - x_{-4})(1 - x_1)} = \frac{(a-b)(c-d)}{(a-c)(b-d)} = \chi(A, B, C, D) = x'_0,$$

which is precisely Equation (20). □

Next, we provide a formula for the inverse of T_3.

Proposition 5.3. *The map $T_3 : \mathcal{P}_n \dashrightarrow \mathcal{P}_n$ is birational. Its inverse is given by*

$$\begin{cases} x_{2i} = x'_{2i+2} \cdot \dfrac{(x'_{2i+4} + x'_{2i+1} - 1)}{x'_{2i+1}x'_{2i+2} - (1 - x'_{2i-1})(1 - x'_{2i+4})}; \\ x_{2i+1} = x'_{2i-1} \cdot \dfrac{(x'_{2i-3} + x'_{2i} - 1)}{x'_{2i}x'_{2i-1} - (1 - x'_{2i+2})(1 - x'_{2i-3})}. \end{cases} \tag{24}$$

We will give an algebraic proof. Consider two families of rational maps $\{\mu_{(s,t)} : \mathbb{R}^{2n} \dashrightarrow \mathbb{R}^{2n}\}_{(s,t)\in\mathbb{Z}^2}$ and $\{\nu_{(s,t)} : \mathbb{R}^{2n} \dashrightarrow \mathbb{R}^{2n}\}_{(s,t)\in\mathbb{Z}^2}$. Write $(a_0, \dots, a_{2n-1}) = \mu_{(s,t)}(x_0, \dots, x_{2n-1})$ and $(b_0, \dots, b_{2n-1}) = \nu_{(s,t)}(x_0, \dots, x_{2n-1})$. Then, we set

$$\begin{cases} a_{2i} = \dfrac{1 - x_{2i+s}}{x_{2i+s+t}} \\ a_{2i+1} = \dfrac{1 - x_{2i+1-s}}{x_{2i+1-s-t}}; \end{cases} \qquad \begin{cases} b_{2i} = \dfrac{1 - x_{2i+s}}{1 - x_{2i+s}x_{2i+s+t}} \\ b_{2i+1} = \dfrac{1 - x_{2i+1-s}}{1 - x_{2i+1-s}x_{2i+1-s-t}}. \end{cases} \tag{25}$$

Lemma 5.4. *Let $\varphi : \mathbb{Z}^2 \to \mathbb{Z}^2$ be the map given by*

$$\varphi(s,t) = ((-1)^{s+1}s,\ (-1)^s(2s+t)). \tag{26}$$

Then, φ is an involution. Moreover, when t is odd, $\mu_{(s,t)}^{-1} = \nu_{\varphi(s,t)}$ and $\nu_{(s,t)}^{-1} = \mu_{\varphi(s,t)}$.

Proof. To see φ is an involution, a direct computation shows that

$$\begin{aligned}\varphi^2(s,t) &= \varphi((-1)^{s+1}s,\ (-1)^s(2s+t)) \\ &= \Big((-1)^{(-1)^{s+1}s+s+2}s,\ (-1)^{(-1)^{s+1}s}\,(2(-1)^{s+1}s + (-1)^s(2s+t))\Big) = (s,t).\end{aligned}$$

Next, we show that when t is odd, $\mu_{(s,t)}^{-1} = \nu_{\varphi(s,t)}$. We will show by direct computation that $\mu_{(s,t)} \circ \nu_{\varphi(s,t)}$ is the identity on the $2i$-th coordinate when s is even. First, when s is even, $\varphi(s,t) = (-s, 2s+t)$. The $2i$-th coordinate of $\mu_{(s,t)} \circ \nu_{\varphi(s,t)}$ is given by

$$\begin{aligned}&\left(1 - \frac{1 - x_{2i+s+(-s)}}{1 - x_{2i+s+(-s)}x_{2i+s+(-s)+(2s+t)}}\right) \cdot \left(\frac{1 - x_{2i+s+t-(-s)}}{1 - x_{2i+s+t-(-s)}x_{2i+s+t-(-s)-(2s+t)}}\right)^{-1} \\ &= \left(1 - \frac{1 - x_{2i}}{1 - x_{2i}x_{2i+2s+t}}\right)\left(\frac{1 - x_{2i+2s+t}x_{2i}}{1 - x_{2i+2s+t}}\right) = x_{2i}.\end{aligned}$$

This is precisely what we want. One can similarly carry out the computation of $\nu_{\varphi(s,t)} \circ \mu_{s,t}$ for the $(2i+1)$-th coordinate, and s odd. We will omit these heavy computations and conclude that $\mu_{(s,t)}^{-1} = \nu_{\varphi(s,t)}$. Finally, to see $\nu_{(s,t)}^{-1} = \mu_{\varphi(s,t)}$, observe that $(-1)^s(2s+t)$ is odd iff t is odd. Therefore, $\nu_{s,t} \circ \mu_{\varphi(s,t)} = \nu_{\varphi^2(s,t)} \circ \mu_{\varphi(s,t)}$ is the identity map by the previous argument. The same argument shows that $\mu_{\varphi(s,t)} \circ \nu_{(s,t)}$ is the identity. □

The following corollary is immediate. We omit the proof.

Corollary 5.5. *For all $(s,t) \in \mathbb{Z}^2$ such that t is odd, $\mu_{(s,t)}$ and $\nu_{(s,t)}$ are birational maps.*

Proof of Proposition 5.3. We first claim that $T_3 = \nu_{(-1,-1)} \circ \mu_{(3,-3)}$. We will provide the computation for even coordinates. Let $(a_0, \dots, a_{2n-1})$ denote the image of $(x_0, \dots, x_{2n-1})$ under $\mu_{(3,-3)}$, and let $(b_0, \dots, b_{2n-1})$ denote the image of $(a_0, \dots, a_{2n-1})$ under $\nu_{(-1,-1)}$. Then, we have

$$\begin{aligned}b_{2i} = \frac{1 - a_{2i-1}}{1 - a_{2i-1}a_{2i-2}} &= \left(1 - \frac{1 - x_{2i-4}}{x_{2i-1}}\right) \cdot \left(1 - \frac{(1 - x_{2i-4})(1 - x_{2i+1})}{x_{2i-1}x_{2i-2}}\right)^{-1} \\ &= \frac{x_{2i-2}(x_{2i-1} + x_{2i-4} + 1)}{x_{2i-1}x_{2i-2} - (1 - x_{2i-4})(1 - x_{2i+1})}.\end{aligned}$$

Observe that this is precisely the first line of (19). The computation for b_{2i+1} is analogous, thus omitted. Then, by Corollary 5.5, $T_3^{-1} = \nu_{(3,-3)} \circ \mu_{(-1,3)}$. Finally, Equation (24) follows from a direct computation of $\nu_{(3,-3)} \circ \mu_{(-1,3)}$ using Equation (25), which we will omit. □

5.2 Conjugated Corner Invariants and Its T_3 Formula

To relate Equation (19) to parameters $(y_r)_{r \in \mathbb{Z}^2}$ in [GP16], it is convenient to consider another coordinate system of $\mathcal{P}_n$, which we define below.

Definition 5.6. Given $[P] \in \mathcal{P}_n$, define the *conjugated corner invariants* to be coordinate functions $\tilde{x}_0(P), \dots, \tilde{x}_{2n-1}(P)$ given by $\tilde{x}_j(P) = \frac{x_j(P)}{x_j(P)-1}$.

The conjugated corner invariants can be viewed as the image of the corner invariants under a birational map $\lambda : \mathbb{R}^{2n} \dashrightarrow \mathbb{R}^{2n}$ sending each coordinate $x_j \longmapsto \frac{x_j}{x_j-1}$. Observe that λ^2 restricted to the dense open set $(\mathbb{R} - \{0,1\})^{2n}$ is the identity map, so $\tilde{x}_j(P)$ is also a coordinate system for $\mathcal{P}_n$. Geometrically, the map λ corresponds to a different choice of permutation in the cross-ratio.

Throughout this section, we will use $\tilde{x}_j = \tilde{x}_j(P)$ and $\tilde{x}'_j = \tilde{x}_j(P')$ to denote the conjugate corner invariants of P and P'. We start by observing some symmetries of conjugating our factorization maps $\mu_{(s,t)}$ and $\nu_{(s,t)}$ from Equation (25).

Lemma 5.7. *For all $(s,t) \in \mathbb{Z}^2$, we have $\lambda \circ \mu_{(s,t)} \circ \lambda = \nu_{(s+t,-t)}$.*

Proof. We can check this by direct computation. We show that the equation holds on even coordinates. The $2i$-th coordinate of $\mu_{(s,t)} \circ \lambda$ is given by

$$\frac{1 - x_{2i+s} \cdot (x_{2i+s} - 1)^{-1}}{x_{2i+s+t} \cdot (x_{2i+s+t} - 1)^{-1}} = \frac{1 - x_{2i+s+t}}{x_{2i+s+t}(x_{2i+s} - 1)}$$

The $2i$-th coordinate of $\lambda \circ \mu_{(s,t)} \circ \lambda$ is given by

$$\left(\frac{1 - x_{2i+s+t}}{x_{2i+s+t}(x_{2i+s} - 1)}\right) \cdot \left(\frac{1 - x_{2i+s+t}}{x_{2i+s+t}(x_{2i+s} - 1)} - 1\right)^{-1} = \frac{1 - x_{2i+s+t}}{1 - x_{2i+s+t}x_{2i+s}},$$

which is precisely the $2i$-th coordinate of $\nu_{(s+t,-t)}$. The computation for the odd coordinates is similar. □

Since λ is an involution, it immediately follows that $\lambda\circ\nu_{(s,t)}\circ\lambda = \mu_{(s+t,-t)}$. This allows us to obtain a formula for T_3 with respect to the conjugated corner invariants.

Proposition 5.8. *Given any 3-nice twisted n-gon P, the following formula holds (indices taken modulo $2n$):*

$$\begin{cases} \tilde{x}'_{2i} = \tilde{x}_{2i-2} \cdot \dfrac{(1-\tilde{x}_{2i-1}\tilde{x}_{2i-4})(1-\tilde{x}_{2i+1})}{(1-\tilde{x}_{2i+1}\tilde{x}_{2i-2})(1-\tilde{x}_{2i-1})}; \\ \tilde{x}'_{2i+1} = \tilde{x}_{2i+3} \cdot \dfrac{(1-\tilde{x}_{2i+2}\tilde{x}_{2i+5})(1-\tilde{x}_{2i})}{(1-\tilde{x}_{2i}\tilde{x}_{2i+3})(1-\tilde{x}_{2i+2})}. \end{cases} \tag{27}$$

Proof. From the proof of Proposition 5.3, we saw that the formula for T_3 on the corner invariants is given by $\nu_{(-1,-1)}\circ\mu_{(3,-3)}$. It follows that the formula for conjugated corner invariants is $\lambda\circ\left(\nu_{(-1,-1)}\circ\mu_{(3,-3)}\right)\circ\lambda$. By Lemma 5.7,

$$\lambda\circ\left(\nu_{(-1,-1)}\circ\mu_{(3,-3)}\right)\circ\lambda = \left(\lambda\circ\nu_{(-1,-1)}\circ\lambda\right)\circ\left(\lambda\circ\mu_{(3,-3)}\circ\lambda\right) = \mu_{(-2,1)}\circ\nu_{(0,3)}.$$

It remains to check that $\mu_{(-2,1)}\circ\nu_{(0,3)}$ agrees with Equation (27). The $2i$-th coordinate of $\mu_{(-2,1)}\circ\nu_{(0,3)}$ is given by

$$\left(1-\frac{1-\tilde{x}_{2i-2}}{1-\tilde{x}_{2i-2}\tilde{x}_{2i+1}}\right)\cdot\left(\frac{1-\tilde{x}_{2i-1}}{1-\tilde{x}_{2i-1}\tilde{x}_{2i-4}}\right)^{-1} = \frac{\tilde{x}_{2i-2}(1-\tilde{x}_{2i-1}\tilde{x}_{2i-4})(1-\tilde{x}_{2i+1})}{(1-\tilde{x}_{2i-2}\tilde{x}_{2i+1})(1-\tilde{x}_{2i-1})}.$$

This is precisely $\tilde{x}'_{2i}$ from Equation (27). The computation for odd coordinates is omitted. □

Using Lemma 5.4, we can easily compute the formula of T_3^{-1} with respect to the conjugated corner invariants. The proof is again a direct computation, so we omit it.

Corollary 5.9. *The formula for T_3^{-1} with conjugated corner invariants is given by $\mu_{(0,3)}\circ\nu_{(2,-3)}$. More specifically,*

$$\begin{cases} \tilde{x}_{2i} = \tilde{x}'_{2i+2} \cdot \dfrac{(1-\tilde{x}'_{2i+1}\tilde{x}'_{2i+4})(1-\tilde{x}'_{2i-1})}{(1-\tilde{x}'_{2i-1}\tilde{x}'_{2i+2})(1-\tilde{x}'_{2i+1})}; \\ \tilde{x}_{2i+1} = \tilde{x}'_{2i-1} \cdot \dfrac{(1-\tilde{x}'_{2i}\tilde{x}'_{2i-3})(1-\tilde{x}'_{2i+2})}{(1-\tilde{x}'_{2i+2}\tilde{x}'_{2i-1})(1-\tilde{x}'_{2i})}. \end{cases} \tag{28}$$

5.3 Relation to Y-Variables

In this section, we discuss how Equation (18) generalizes the results from [GP16]. The propositions in this section hold for all four cells $S_n(I,J)$, $S_n(J,I)$, $S_n(K,J)$, $S_n(J,K)$. For notational convenience, our statements will only mention $S_n(J,I)$. The readers may assume that the propositions hold for the other three cells with the same proof.

The map T_3 along with the labeling convention of Equation (18) corresponds to the following construction in [GP16]. Let $a,b,c,d \in \mathbb{Z}^2$ be distinct and assume $a_2 \le b_2 \le c_2 \le d_2$. Say that $S = \{a,b,c,d\}$ is a *Y-pin* if $b_2 < c_2$ and the vectors $b-a$, $c-a$, $d-a$ generate all of $\mathbb{Z}^2$.

Definition 5.10 ([GP16, Definition 1.4])**.** Let $S = \{a,b,c,d\}$ be a Y-pin and suppose $D \ge 2$. A *Y-mesh of type S and dimension D* is a grid of points $\hat{P}_{i,j}$ in $\mathbb{RP}^D$ with $i,j \in \mathbb{Z}$ which together span all of $\mathbb{RP}^D$ and such that

- $\hat{P}_{r+a}, \hat{P}_{r+b}, \hat{P}_{r+c}, \hat{P}_{r+d}$ are distinct for all $r \in \mathbb{Z}^2$.
- Let $L_r = \hat{P}_{r+a}\hat{P}_{r+b}$. Then, $\hat{P}_{r+a}, \hat{P}_{r+b}, \hat{P}_{r+c}, \hat{P}_{r+d}$ all lie on L_r for all $r \in \mathbb{Z}^2$.
- The four lines $L_{r-a}, L_{r-b}, L_{r-c}, L_{r-d}$ (all of which contain $\hat{P}_r$) are distinct for all $r \in \mathbb{Z}^2$.

Let $S = \{(-1,0),(2,0),(0,1),(1,1)\}$, which is a Y-pin. Given a representative P of some $[P] \in S_n(J,I)$, we can consider a grid $(\hat{P}_{i,j})_{(i,j)\in\mathbb{Z}^2}$ where $\hat{P}_{i,j}$ is the i-th vertex of $T_3^j(P)$.

Proposition 5.11. *$(\hat{P}_{i,j})$ is a Y-mesh of type S and dimension 2.*

Proof. The first two conditions of Definition 5.10 are straightforward to verify using the identification $S_n(J,I) = \mathcal{S}^{\alpha}_{3,n}$ from Proposition 4.10. For the third condition, let $P^{(j)} = T_3^j(P)$. Then, we have

$$L_{r-a} = P^{(j)}_{i-1}P^{(j)}_{i+2}, \quad L_{r-b} = P^{(j)}_{i-1}P^{(j)}_{i-4}, \quad L_{r-c} = P^{(j)}_{i-1}P^{(j)}_{i}, \quad L_{r-d} = P^{(j)}_{i-1}P^{(j)}_{i-2}.$$

Notice also that $L_{r-a} = P^{(j+1)}_{i}P^{(j+1)}_{i+1}$ and $L_{r-b} = P^{(j+1)}_{i-2}P^{(j+1)}_{i-1}$, so 3-niceness of $P^{(j+1)}$ implies they are distinct. The other pairings are distinct because of 3-niceness of $P^{(j)}$. □

[GP16] then introduces the parameters $y_r(\hat{P})$ associated to a Y-mesh. Fix a Y-pin $S = \{a, b, c, d\}$ and a Y-mesh $\hat{P}$ of type S and dimension D. For all $r \in \mathbb{Z}^2$, consider

$$y_r(\hat{P}) = -\chi(\hat{P}_{r+a}, \hat{P}_{r+c}, \hat{P}_{r+d}, \hat{P}_{r+b}). \tag{29}$$

See the left side of Figure 23 for the setup using the Y-mesh from Proposition 5.11. [GP16, Theorem 1.6] give us the following relation on y_r:

$$y_{i+1,j}\, y_{i+1,j+2} = \frac{(1 + y_{i-1,j+1})(1 + y_{i+3,j+1})}{(1 + y_{i,j+1}^{-1})(1 + y_{i+2,j+1}^{-1})}. \tag{30}$$

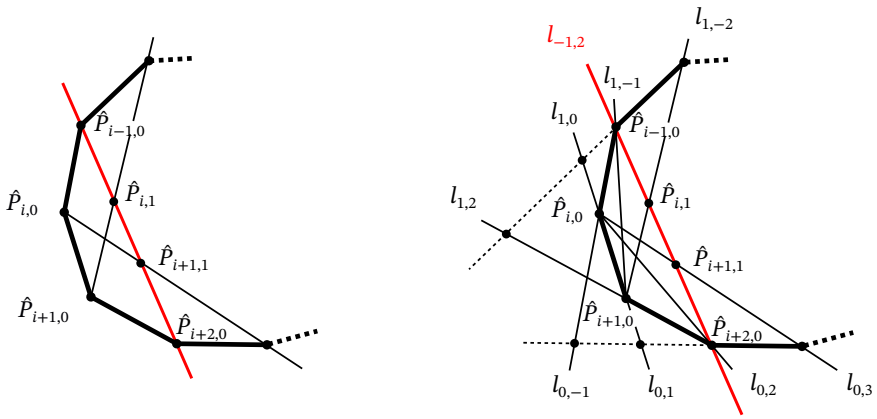

Figure 23: Left: Definition of $y_r(\hat{P})$ for the Y-mesh from Proposition 5.11. Right: Relationship between $y_r(\hat{P})$ and conjugated corner invariants.

Lemma 5.12. *Given a representative P of $[P] \in S_n(I, J)$ with conjugated corner invariants $\tilde{x}_j = \tilde{x}_j(P)$. Let $(\hat{P}_{i,j})$ be its corresponding Y-mesh with $y_r = y_r(\hat{P})$ for all $r \in \mathbb{Z}^2$. Then, for all $i \in \mathbb{Z}$,*

$$y_{i,0} = -\tilde{x}_{2i}\tilde{x}_{2i+3}. \tag{31}$$

Proof. Let $l_{a,b} = P_{i+a}P_{i+b}$. See right side of Figure 23 for the setup. Equation (8) gives us

$$\tilde{x}_{2i} = \frac{x_{2i}}{x_{2i} - 1} = \chi(l_{1,-2}, l_{1,-1}, l_{1,2}, l_{1,0}); \quad \tilde{x}_{2i+3} = \frac{x_{2i+3}}{x_{2i+3} - 1} = \chi(l_{0,3}, l_{0,2}, l_{0,-1}, l_{0,1}).$$

Notice that $(l_{1,-1} \cap l_{0,-1}) \cap (l_{1,2} \cap l_{0,2}) = P_{i-1}P_{i+2} = l_{-1,2}$. Then, from elementary cross ratio identities we have

$$\begin{aligned}\tilde{x}_{2i}\tilde{x}_{2i+3} &= \chi(l_{1,-1} \cap l_{-1,2}, l_{1,-2} \cap l_{-1,2}, l_{0,3} \cap l_{-1,2}, l_{0,2} \cap l_{-1,2}) \\ &= \chi(\hat{P}_{i-1,0}, \hat{P}_{i,1}, \hat{P}_{i+1,1}, \hat{P}_{i+2,0}) = -y_{i,0},\end{aligned}$$

which is precisely Equation (31). □

Remark 5.13. Equation (31) is very similar to the correspondence of y_r and corner invariants in the T_2 case. Let P be an arbitrary twisted n-gon with $P' = T_2(P)$. If we use the labeling convention $P'_i = P_{i-1}P_{i+1} \cap P_iP_{i+2}$, then the T_2-orbit $(\hat{P}_{i,j})_{(i,j)\in\mathbb{Z}^2}$, where $\hat{P}_{i,j}$ is the i-th vertex of $T_2^j(P)$, is a Y-mesh of type $S = \{(-1,0),(1,0),(-1,1),(0,1)\}$. Denote by $x_j = x_j(P)$ the corner invariants of P. Then, for all $i \in \mathbb{Z}$,

$$y_{i,0} = -x_{2i+1}x_{2i+2}. \tag{32}$$

For the proof of Equation (32), see [Gli11, Equation (2.2)].

Theorem 5.14. *For the Y-pin $S = \{(-1,0),(2,0),(0,1),(1,1)\}$, the transformation formula of y_r from* [GP16, Theorem 1.6] *is a direct consequence of the birational formula for the conjugated corner invariants under T_3.*

Proof. It suffices to show that we can use Equation (31) to derive (30) for $j = -1$. We first compute $y_{i+1,-1}$ and $y_{i+1,1}$ using Equation (27) and (28):

$$\begin{aligned} y_{i+1,-1} &= -\frac{\tilde{x}_{2i+4}(1-\tilde{x}_{2i+3}\tilde{x}_{2i+6})(1-\tilde{x}_{2i+1})}{(1-\tilde{x}_{2i+1}\tilde{x}_{2i+4})(1-\tilde{x}_{2i+3})} \cdot \frac{\tilde{x}_{2i+3}(1-\tilde{x}_{2i+1}\tilde{x}_{2i+4})(1-\tilde{x}_{2i+6})}{(1-\tilde{x}_{2i+3}\tilde{x}_{2i+6})(1-\tilde{x}_{2i+4})} \\ &= -\frac{\tilde{x}_{2i+3}\tilde{x}_{2i+4}(1-\tilde{x}_{2i+1})(1-\tilde{x}_{2i+6})}{(1-\tilde{x}_{2i+3})(1-\tilde{x}_{2i+4})}; \\ y_{i+1,1} &= -\frac{\tilde{x}_{2i}(1-\tilde{x}_{2i-2}\tilde{x}_{2i+1})(1-\tilde{x}_{2i+3})}{(1-\tilde{x}_{2i}\tilde{x}_{2i+3})(1-\tilde{x}_{2i+1})} \cdot \frac{\tilde{x}_{2i+7}(1-\tilde{x}_{2i+6}\tilde{x}_{2i+9})(1-\tilde{x}_{2i+4})}{(1-\tilde{x}_{2i+4}\tilde{x}_{2i+7})(1-\tilde{x}_{2i+6})} \\ &= -\frac{\tilde{x}_{2i}\tilde{x}_{2i+7}(1+y_{i-1,0})(1+y_{i+3,0})(1-\tilde{x}_{2i+3})(1-\tilde{x}_{2i+4})}{(1+y_{i,0})(1+y_{i+2,0})(1-\tilde{x}_{2i+1})(1-\tilde{x}_{2i+6})}. \end{aligned} \tag{33}$$

It follows that

$$\begin{aligned} y_{i+1,-1}\,y_{i+1,1} &= \frac{\tilde{x}_{2i}\tilde{x}_{2i+3}\tilde{x}_{2i+4}\tilde{x}_{2i+7}(1+y_{i-1,0})(1+y_{i+3,0})}{(1+y_{i,0})(1+y_{i+2,0})} \\ &= \frac{y_{i,0}y_{i+2,0}(1+y_{i-1,0})(1+y_{i+3,0})}{(1+y_{i,0})(1+y_{i+2,0})} = \frac{(1+y_{i-1,0})(1+y_{i+3,0})}{(1+y_{i,0}^{-1})(1+y_{i+2,0}^{-1})}. \end{aligned}$$

This concludes the proof. □

6 The Precompactness of T_3 Orbits

In this section, we establish four algebraic invariants of T_3. We then use them to prove Theorem 1.3. Having Theorem 4.6 in hand, we may fully work with $S_n(J,I)$ and $S_n(K,J)$. Our strategy is to use the algebraic invariants to show that the corner invariants are uniformly bounded.

6.1 The Four Invariants

Proposition 6.1. *Given $[P] \in \mathcal{P}_n$ with corner invariants $x_j = x_j(P)$, consider the following four quantities $\mathcal{F}_i = \mathcal{F}_i(P)$:*

$$\mathcal{F}_1 = \prod_{i=0}^{n-1} \frac{x_{2i}}{x_{2i}-1}; \quad \mathcal{F}_2 = \prod_{i=0}^{n-1} \frac{x_{2i+1}}{x_{2i+1}-1}; \quad \mathcal{F}_3 = \prod_{i=0}^{n-1} \frac{x_{2i}}{x_{2i+1}}; \quad \mathcal{F}_4 = \prod_{i=0}^{n-1} \frac{1-x_{2i}}{1-x_{2i+1}}. \tag{34}$$

Then, $\mathcal{F}_i$ is invariant under T_3 for $i = 1,2,3,4$.

Proof. We first show that $\mathcal{F}_3$ is invariant under T_3. Let $\mathcal{F}_3'$ denote the invariants obtained by plugging in x_i' from Equation (24). Observe that

$$\begin{aligned}\mathcal{F}_3' &= \mathcal{F}_3 \cdot \prod_{i=0}^{n-1} \frac{x_{2i-4}+x_{2i-1}-1}{x_{2i+2}+x_{2i+5}-1} \cdot \prod_{i=0}^{n-1} \frac{x_{2i+2}x_{2i+3}-(1-x_{2i+5})(1-x_{2i})}{x_{2i-2}x_{2i-1}-(1-x_{2i+1})(1-x_{2i-4})} \\ &= \mathcal{F}_3 \cdot \frac{\prod_{i=-3}^{n-4}(x_{2i+2}+x_{2i+5}-1)}{\prod_{i=0}^{n-1}(x_{2i+2}+x_{2i+5}-1)} \cdot \frac{\prod_{i=2}^{n+1}(x_{2i-2}x_{2i-1}-(1-x_{2i+1})(1-x_{2i-4}))}{\prod_{i=0}^{n-1}(x_{2i-2}x_{2i-1}-(1-x_{2i+1})(1-x_{2i-4}))} = \mathcal{F}_3.\end{aligned}$$

This shows $\mathcal{F}_3' = \mathcal{F}_3$. Next, we show that $\mathcal{F}_1$ and $\mathcal{F}_2$ are invariant. Using conjugated corner invariants, we see that $\mathcal{F}_1 = \prod_{i=0}^{n-1} \tilde{x}_{2i}$ and $\mathcal{F}_2 = \prod_{i=0}^{n-1} \tilde{x}_{2i+1}$. We let $\mathcal{F}_1' = \prod_{i=0}^{n-1} \tilde{x}_{2i}'$ be the first invariant of $T_3(P)$. Equation (27) gives us

$$\mathcal{F}_1' = \mathcal{F}_1 \cdot \prod_{i=0}^{n-1} \frac{(1-\tilde{x}_{2i-1}\tilde{x}_{2i-4})(1-\tilde{x}_{2i+1})}{(1-\tilde{x}_{2i+1}\tilde{x}_{2i-2})(1-\tilde{x}_{2i-1})} = \mathcal{F}_1,$$

where the last equality follows from cyclically permuting the numerator. This shows $\mathcal{F}_1' = \mathcal{F}_1$. The proof for $\mathcal{F}_2$ goes through the same computation, so we omit it.

Finally, observe that $\mathcal{F}_4 = \frac{\mathcal{F}_2\mathcal{F}_3}{\mathcal{F}_1}$, so by invariance of $\mathcal{F}_1, \mathcal{F}_2, \mathcal{F}_3$, we know that $\mathcal{F}_4$ must also be invariant. This concludes the proof. □

Remark 6.2. As shown in the proof of Proposition 6.1, $\mathcal{F}_1$ and $\mathcal{F}_2$ correspond to the product of conjugated corner invariants. $\mathcal{F}_3$ is the ratio of the two Casimirs $\frac{O_n}{E_n}$ of the T_2 invariant Poisson structure on $\mathcal{P}_n$. For discussions on $\mathcal{F}_3$ and the Casimirs, see [Sch24, §2.3]. Also, since $\mathcal{F}_1\mathcal{F}_4 = \mathcal{F}_2\mathcal{F}_3$, the four T_3 invariants are not algebraically independent.

Below is a direct consequence of the invariance of the $\mathcal{F}_i$'s. Since the $\mathcal{F}_i$'s are preserved by the forward action, it must also be preserved by the backward action.

Corollary 6.3. *The four invariants $\mathcal{F}_1, \mathcal{F}_2, \mathcal{F}_3, \mathcal{F}_4$ are also invariant under T_3^{-1}.*

6.2 Proof of Theorem 1.3

Recall that a subset A of a topological space X is precompact if the closure of A is compact. To show that the T_3-orbit is precompact, it suffices to show that the corner invariants of the orbit are uniformly bounded away from the singularities $0, 1, \infty$.

In this section, we let $[n] := \{1, \dots, n\}$. Given $[P] \in \mathcal{P}_n$, for all $j, m \in \mathbb{Z}$, let $x_{j,m} = x_j(T_3^m(P))$ whenever $T_3^m(P)$ exists. Let $\mathcal{F}_{i,m} = \mathcal{F}_i(T_3^m(P))$ for $i = 1, 2, 3, 4$. By Proposition 6.1, $\mathcal{F}_{i,m}$ is independent of m. All sequences are indexed by $\mathbb{Z}_{\geq 0}$ unless specified otherwise. Finally, when we say "$\{a_m\}$ converges/diverges on a subsequence, and $\{b_m\}$ converges/diverges on the same subsequence," we mean that a subsequence of $\{b_m\}$ with the same choice of indices as the subsequence of $\{a_m\}$ converges/diverges.

Lemma 6.4. *Given $[P] \in S_n(J, I)$, there exist $a, b \in J$ such that $x_{2i,m} \in [a, b]$ for all $i \in [n]$ and $m \in \mathbb{Z}_{\geq 0}$.*

Proof. We first claim that for each i, the sequence $\{x_{2i,m}\}$ is bounded above uniformly by some $b_i \in J$. If not, then $x_{2i,m} \to 1$ on a subsequence, which implies $1 - x_{2i,m} \to 0$ on the

same subsequence. Since $[T_3^m(P)] \in S_n(J,I)$ for all $m \in \mathbb{Z}_{\geq 0}$, we must have $1 - x_{2j,m} \in (0,1)$ and $(1 - x_{2j+1,m})^{-1} \in (0,1)$ for all $j \in [n]$. This implies $\mathcal{F}_{4,m} \to 0$ on the same subsequence, but that contradicts invariance of $\mathcal{F}_{4,m}$. Therefore, $\{x_{2i,m}\}$ is bounded above by $b_i = \sup_m\{x_{2i,m}\} \in J$. Taking $b = \max_{i\in[n]} b_i$ satisfies the condition in the lemma.

Next, we show $\{x_{2i,m}\}$ is bounded below uniformly by some $a_i > 0$. If not, then $x_{2i,m} \to 0$ on a subsequence, so $x_{2i,m} \cdot (x_{2i,m} - 1)^{-1} \to 0$ on the same subsequence. From the argument above, $x_{2j,m} \leq b$ for all $m \in \mathbb{Z}_{\geq 0}$ and $j \in [n]$, which gives us $|x_{2j,m} \cdot (x_{2j,m} - 1)^{-1}| \leq |\frac{b}{b-1}|$, so the sequences are uniformly bounded for all $j \neq i$. This together with $|x_{2i,m} \cdot (x_{2i,m} - 1)^{-1}| \to 0$ on a subsequence implies $|\mathcal{F}_{1,m}| \to 0$ on the same subsequence, but that contradicts invariance of $\mathcal{F}_{1,m}$. Therefore, $\{x_{2i,m}\}$ is bounded below by $a_i = \inf_m\{x_{2i,m}\} \in J$. Taking $a = \min_{i\in[n]} a_i$ completes the proof. □

Lemma 6.5. *With the same notation as in Lemma 6.6, there exist $c, d \in I$ such that $x_{2i+1,m} \in [c,d]$ for all $i \in [n]$ and $m \in \mathbb{Z}_{\geq 0}$.*

Proof. We first claim that for each i,the sequence $\{x_{2i+1,m}\}$ is bounded above uniformly by some $d_i \in I$. If not, then, $x_{2i+1,m} \cdot (x_{2i+1,m} - 1)^{-1} \to 0$ on a subsequence. Since $x_{2j+1,m} \cdot (x_{2j+1,m} - 1)^{-1} \in (0,1)$ for all $j \in [n]$, we must have $\mathcal{F}_{2,m} \to 0$ on the same subsequence, but that contradicts invariance of $\mathcal{F}_{2,m}$.

Next, we show that $\{x_{2i+1,m}\}$ is bounded below uniformly by some $c_i \in I$. If not, then a subsequence of $\{x_{2i+1,m}\}$ must diverge, so the same subsequence of $\{1 - x_{2i+1,m}\}$ also diverges. Lemma 6.4 and $x_{2i+1,m} \leq d_i < 0$ together implies $\mathcal{F}_{4,m}$ diverges on the same subsequence, but that contradicts invariance of $\mathcal{F}_{4,m}$. Finally, taking $c = \min_{i\in[n]} c_i$ and $d = \max_{i\in[n]} d_i$ completes the proof. □

The proofs of the following two lemmas are analogous to Lemma 6.4 and 6.5. We will omit the details and point out which invariants to use in each step.

Lemma 6.6. *Given $[P] \in S_n(K,J)$, there exist $a, b \in J$ such that $x_{2i+1,m} \in [a,b]$ for all $i \in [n]$ and $m \in \mathbb{Z}_{\geq 0}$.*

Proof. For each i, the sequence $\{x_{2i+1,m}\}$ is bounded below by some $a_i \in J$, for otherwise $\mathcal{F}_{3,m}$ diverges on a subsequence. Next, since $\{|\mathcal{F}_{3,m}|\}$ is bounded below by $\prod_{j=0}^{n-1} a_j > 0$, $\{x_{2i+1,m}\}$ is bounded above by some $b_i \in J$. Taking $a = \min_{i\in[n]} a_i$ and $b = \max_{i\in[n]} b_i$ completes the proof. □

Lemma 6.7. *With the same notation as in Lemma 6.6, there exist $c, d \in K$ such that $x_{2i,m} \in [c, d]$ for all $i \in [n]$ and $m \in \mathbb{Z}_{\geq 0}$.*

Proof. For each i, the sequence $\{x_{2i,m}\}$ must be bounded below by some $c_i \in K$, for otherwise $\mathcal{F}_{1,m} \to \infty$ on a subsequence. It's also bounded above by some d_i. To see this, Lemma 6.6 implies all corner invariants are bounded away from 0, so if $\{x_{2i,m}\}$ is not bounded above, then $\mathcal{F}_{3,m}$ diverges on a subsequence. Taking $c = \min_i c_i$ and $d = \max_i d_i$ completes the proof. □

Proof of Theorem 1.3. We will show that the forward T_3 orbit of $[P] \in \mathcal{S}^{\alpha}_{3,n} = S_n(J, I)$ has uniformly bounded corner invariants. By Proposition 4.10, $[P] \in S_n(J, I)$. Let $[a, b] \subset J$, $[c, d] \subset I$ be compact intervals derived from Lemma 6.4 and 6.5. Then, the sequence $\{(x_{0,m}, \dots, x_{2n-1,m})\}$ is contained in $\prod_{i=0}^{n-1}[a, b] \times [c, d]$, so it is uniformly bounded. To show precompactness of the backward T_3 orbit of $\mathcal{S}^{\alpha}_{3,n}$, one can adapt the proofs of Lemma 6.4 and 6.5 with very few changes. We omit the details. The case $\mathcal{S}^{\beta}_{3,n}$ follows from Lemma 6.6 and 6.7 by essentially the same argument, which we again omit. □

7 Type-β 2-Spirals and Precompact T_2 Orbits

7.1 The Corner Invariants of Type-β 2-Spirals

We finish this paper by discussing the type-β 2-spirals. Proposition 3.10 implies $\mathcal{S}^{\beta}_{2,n}$ is disjoint from the moduli space of closed convex polygons, so $\mathcal{S}^{\beta}_{2,n}$ is a new invariant geometric construction under the pentagram map by Theorem 1.1. In this section, we analyze the corner invariants of $\mathcal{S}^{\beta}_{2,n}$ and show that just like the type-α and type-β 3-spirals, it is cut out by linear boundaries.

Proposition 7.1. *For all $n \geq 2$, given any $[P] \in \mathcal{S}^{\beta}_{2,n}$ with corner invariants $x_j = x_j(P)$, we have $x_{2i} > 0$ and $x_{2i+1} < 0$ for all $i \in [n]$.*

Proof. Let P be an $(i-2)$-representative of $[P]$. Normalize by $\mathrm{Aff}^{+}_{2}(\mathbb{R})$ so that $P_{i-1} = (-1, 0)$, $P_i = (0, 0)$, $P_{i+1} = (0, 1)$ on the affine patch, which is possible because (P_{i-1}, P_i, P_{i+1}) is positive. Let $s_{a,b} \in \mathbb{R} \cup \{\infty\}$ denote the slope of $P_{i+a}P_{i+b}$. Positivity of (P_{i-2}, P_{i-1}, P_i) and $P_{i+1} \in \mathrm{int}(P_{i-2}, P_{i-1}, P_i)$ implies $s_{-1,-2} > 1$ and $s_{1,-2} > 1$. Similarly, since $P_{i+2} \in \mathrm{int}(P_{i-1}, P_i, P_{i+1})$, we have $s_{-1,2} \in (0, 1)$ and $s_{1,2} > 1$. It follows that

$$\begin{aligned} x_{2i} &= \frac{(s_{1,-2} - s_{1,-1})(s_{1,0} - s_{1,2})}{(s_{1,-2} - s_{1,0})(s_{1,-1} - s_{1,2})} = -\frac{s_{1,-2} - 1}{1 - s_{1,2}} > 0; \\ x_{2i+1} &= \frac{(s_{-1,2} - s_{-1,1})(s_{-1,0} - s_{-1,-2})}{(s_{-1,2} - s_{-1,0})(s_{-1,1} - s_{-1,-2})} = \frac{-s_{-1,-2}(s_{-1,2} - 1)}{s_{-1,2}(1 - s_{-1,-2})} < 0. \end{aligned} \tag{35}$$

This concludes the proof. □

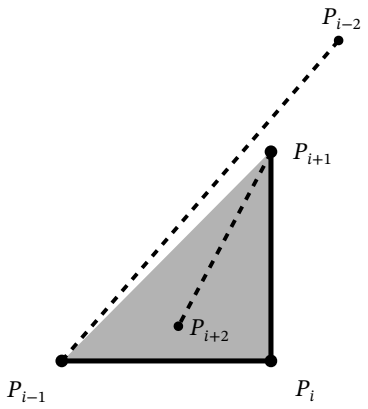

Figure 24: Configuration of Proposition 7.1 and 7.2.

Proposition 7.2. *For all $n \geq 2$, if $[P] \in \mathcal{P}_n$ has corner invariants $x_j = x_j(P)$ such that $x_{2i} > 0$ and $x_{2i+1} < 0$ for all $i \in [n]$, then $[P] \in \mathcal{S}^{\beta}_{2,n}$.*

Proof. Fix $N \in \mathbb{Z}$. Let P be a representative of $[P]$ such that $P_{N-2} = (\frac{1}{3}, \frac{3}{2})$, $P_{N-1} = (-1, 0)$, $P_N = (0, 0)$, and $P_{N+1} = (0, 1)$. We say P satisfies condition $(**)_i$ if (P_{i-1}, P_i, P_{i+1}) is positive and $P_{i+2} \in \mathrm{int}(P_{i-1}, P_i, P_{i+1})$. Then, P is a type-β N-representative of 2-spirals iff P satisfies

$(**)_i$ for all $i > N$. Notice that P satisfies $(**)_N$, so by an induction argument, it suffices to show that for $i \geq N$, if P satisfies $(**)_i$, then P satisfies $(**)_{i+1}$.

If P satisfies $(**)_i$, then (P_{i-1}, P_i, P_{i+1}) is positive. Normalize by $\mathrm{Aff}_2^+(\mathbb{R})$ so that $P_{i-1} = (-1, 0)$, $P_i = (0, 0)$, and $P_i = (0, 1)$. We will use the same notation $l_{a,b}$ and $s_{a,b}$ as Proposition 7.1. Since $P_{i+1} \in \mathrm{int}(P_{i-2}, P_{i-1}, P_i)$, we have $s_{-1,-2} > 1$ and $s_{1,-2} > 1$. Then, since $x_{2i} > 0$ and $x_{2i+1} < 0$, Equation (35) gives us

$$\frac{s_{1,-2} - 1}{s_{1,2} - 1} > 0 \text{ and } \frac{s_{-1,-2}(s_{-1,2} - 1)}{s_{-1,2}(s_{-1,-2} - 1)} < 0.$$

It follows that $s_{1,2} > 1$ and $1 - \frac{1}{s_{-1,2}} < 0$. The latter inequality implies $\frac{1}{s_{-1,2}} > 1$, so in particular $s_{-1,2} > 0$ and hence $s_{-1,2} \in (0, 1)$. The two conditions $s_{1,2} > 1$ and $s_{-1,2} \in (0, 1)$ implies $P_{i+2} \in \mathrm{int}(P_{i-1}, P_i, P_{i+1})$ and (P_i, P_{i+1}, P_{i+2}) positive, so P satisfies $(**)_{i+1}$ as desired. We conclude that $[P] \in \mathcal{S}_{2,n}^{\beta}$. □

7.2 The Precompactness of T_2 Orbits

We adapt the argument for Theorem 1.3 to give a quick proof of Theorem 1.4 using the Casimir functions of the T_2-invariant Poisson structure on $\mathcal{P}_n$ that were developed in [Sch08, Theorem 1.2]. One can find the proof of the following lemma in [Sch08, §2.2].

Lemma 7.3. *For the map T_2 acting on a twisted n-gon P with corner invariants $x_j = x_j(P)$, one has the following four invariant quantities.*

$$O_1(P) = \sum_{i=0}^{n-1}(-x_{2i+1} + x_{2i-1}x_{2i}x_{2i+1}); \quad O_n(P) = \prod_{i=0}^{n-1} x_{2i+1};$$
$$E_1(P) = \sum_{i=0}^{n-1}(-x_{2i} + x_{2i-2}x_{2i-1}x_{2i}); \quad E_n(P) = \prod_{i=1}^{n} x_{2i}.$$

We continue to use the notation from §6.2. In addition, we write $O_{1,m} = O_1(T_2^m(P))$. We define $O_{n,m}$, $E_{1,m}$, and $E_{n,m}$ analogously. By Lemma 7.3, the values of these four quantities are independent of the choice of m.

Lemma 7.4. *For all $n \geq 2$, given $[P] \in \mathcal{S}_{2,n}^{\beta}$, there exists $a, b > 0$ such that $x_{2i,m} \in [a, b]$ for all $i \in [n]$ and $m \in \mathbb{Z}_{\geq 0}$.*

Proof. Fix $i \in [n]$. We first show that $x_{2i,m}$ is uniformly bounded above by some $b > 0$. Since $T_2^m(P) \in \mathcal{S}^{\beta}_{2,n}$ for all $m \in \mathbb{Z}_{\geq 0}$, we must have $E_{1,m} < -x_{2i,m} < 0$. Then, if $x_{2i,m} \to \infty$ on a subsequence, $E_{1,m}$ also diverges on the same subsequence, but that contradicts invariance of $E_{1,m}$. This implies $x_{2i,m} < b_i$ for some $b_i > 0$. Taking $b = \max_{i\in[n]} b_i$ satisfies the condition in the lemma.

Next, we show that $x_{2i,m}$ is uniformly bounded below by some $a > 0$. We first notice that $E_{n,m} < b_i^n$. This implies if $x_{2i,m} \to 0$ on a subsequence, then $E_{n,m} \to 0$ on the same subsequence, but that contradicts invariance of $E_{n,m}$. Therefore, $x_{2i,m} > a_i$ for some $a_i > 0$. Taking $a = \min_{i\in[n]} a_i$ completes the proof. □

Lemma 7.5. *For all $n \geq 2$, given $[P] \in \mathcal{S}^{\beta}_{2,n}$, there exists $c, d < 0$ such that $x_{2i+1,m} \in [c, d]$ for all $i \in [n]$ and $m \in \mathbb{Z}_{\geq 0}$.*

Proof. The argument is analogous to the proof of Lemma 7.4. Fix $i \in [n]$. To find c_i that bounds $\{x_{2i+1,m}\}$ uniformly from below, we use the fact that $O_{1,m} > -x_{2i+1} > 0$. We then set $c = \min_{i\in[n]} c_i$. To find d_i that bounds $\{x_{2i+1,m}\}$ uniformly from above, we use the fact that $|O_n(P)| < |c^n|$. We then set $d = \max_{i\in[n]} d_i$ to complete the proof. □

Lemma 7.4 and 7.5 together implies that the forward T_2-orbit of any $[P] \in \mathcal{S}^{\beta}_{2,n}$ is precompact in $\mathcal{P}_n$. One can use the same argument to show that the backward T_2-orbit is also precompact. We have thus completed the proof of Theorem 1.4.

8 Appendix

8.1 Conjectures for Invariants

Given $[P] \in \mathcal{P}_{k,n}$, we may consider the following quantity:

$$y_i^{(k)}(P) = -\chi(P_i, P_iP_{i+k} \cap P_{i-1}P_{i+k-1}, P_iP_{i+k} \cap P_{i+1}P_{i+k+1}, P_{i+k}). \tag{36}$$

When $T_k^j(P)$ is well-defined, we write $y_{i,j}^{(k)} = y_i^{(k)}(T_k^j(P))$, or simply $y_{i,j}$ if the value of k is clear from the context. Let $Y_j^{(k)}$ (or simply Y_j) denote the product $\prod_{i=0}^{n-1} y_{i,j}^{(k)}$.

Proposition 8.1. *For all $k, n \geq 2$, given $[P] \in \mathcal{S}^{\alpha}_{k,n}$, there exists $C \in \mathbb{R}$, $C \neq 0$, such that*

$$Y^{(k)}_{j+1}\left(Y^{(k)}_{j}\right)^{-1} = C \tag{37}$$

for all $j \in \mathbb{Z}$. The same holds for $[P] \in \mathcal{S}^{\beta}_{k,n}$.

Proof. The grid $(\hat{P}_{i,j})_{(i,j)\in\mathbb{Z}^2}$ where $\hat{P}_{i,j}$ is the i-th vertex of $T^j_k(P)$ is a Y-mesh of type $S = \{(0,0),(k,0),(-1,1),(0,1)\}$ with $y_r = y_r(\hat{P})$ for $r \in \mathbb{Z}^2$. The proof is essentially the same as the one for Proposition 5.11, so we will omit it. Then, from [GP16, Theorem 1.6], we have

$$y_{i+k,j}y_{i-1,j+2} = \frac{(1+y_{i-1,j+1})(1+y_{i+k,j+1})}{(1+y^{-1}_{i,j+1})(1+y^{-1}_{i+k-1,j+1})}. \tag{38}$$

It follows that

$$\begin{aligned} Y_jY_{j+2} &= \prod_{i=0}^{n-1}(y_{i+k,j}y_{i-1,j+2}) = \prod_{i=0}^{n-1}\frac{(1+y_{i-1,j+1})(1+y_{i+k,j+1})}{(1+y^{-1}_{i,j+1})(1+y^{-1}_{i+k-1,j+1})} \\ &= \left(\prod_{i=0}^{n-1}(y_{i,j+1}\,y_{i+k-1,j+1})\right)\left(\prod_{i=0}^{n-1}\frac{(1+y_{i-1,j+1})(1+y_{i+k,j+1})}{(1+y_{i,j+1})(1+y_{i+k-1,j+1})}\right) = Y^2_{j+1}. \end{aligned} \tag{39}$$

This implies $Y_{j+2}/Y_{j+1} = Y_{j+1}/Y_j$ for all $j \in \mathbb{Z}$. Taking $C = Y_1/Y_0$ completes the proof. □

Remark 8.2. Combining the results of [GP16] and [GSTV12], we see that Proposition 8.1 is equivalent to [GSTV12, Theorem 2.1]. Specifically, the quantity in Equation (37) is shown to be a Casimir function with respect to a Poisson structure that is invariant under the y-variable transformation of a quiver Q_k, which we will define below.

Consider the infinite directed graph Q_k whose vertices are indexed by $\mathbb{Z}\times\{0,1\}$, with directed edges $(i,0)\to(i-1,1)$, $(i,0)\to(i-k,1)$, $(i,1)\to(i,0)$, and $(i-k-1,1)\to(i,0)$ for all $i \in \mathbb{Z}$. See Figure 25 for a visual representation of this quiver. We refer the readers to [GP16, §9] for the construction of this quiver and the proof that the y-variable transformations satisfy (38).

For all $n \geq 2$, the y-variables corresponding to $[P] \in \mathcal{P}_{k,n}$ are periodic modulo n. We may then identify vertices of Q_k via $(i,j) \sim (i+n,j)$, and similarly identify the corresponding edges. The resulting directed graph $Q_{k,n}$ is isomorphic to the quiver $\mathcal{Q}_{k,n}$ from [GSTV12]

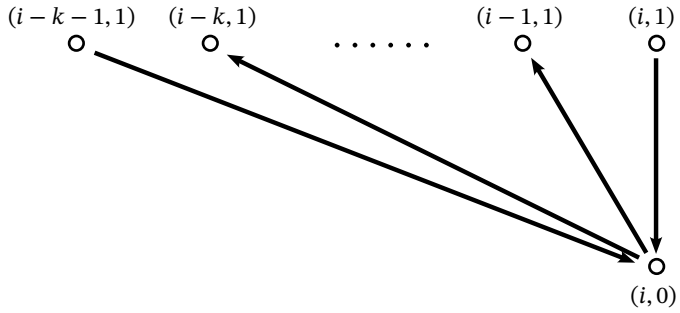

Figure 25: The quiver Q_k. Only edges into and out of the vertex $(i,0)$ are shown.

by applying a translation to the first entry of the vertices $(i,1)$. Moreover, the y-variables $(y_{i,0})_{i\in[n]}$ of the quiver in [GP16] transforms in the same way as the p-variables $(p_i)_{i\in[n]}$ of $\mathcal{Q}_{k,n}$ under the map $\overline{T_k}$ (see [GSTV12, §2]), and the q-variables $(q_i)_{i\in[n]}$ of $\mathcal{Q}_{k,n}$ correspond to the multiplicative inverse of $y_{i,-1}$. As a result, $Y_0^{(k)}/Y_{-1}^{(k)} = \prod_{i=1}^n p_i q_i$, which by [GSTV12, Theorem 2.1] is invariant under $\overline{T_k}$ and forms a Casimir function with respect to a Poisson structure that is invariant under $\overline{T_k}$.

Both [GP16] and [GSTV12] demonstrate that the quiver $Q_{k,n}$ is a bipartite graph that can be embedded into a torus. For further details, see [GP16, §9] and [GSTV12, §3]. This connection links $Q_{k,n}$ to the *Goncharov-Kenyon Dimer Integrable Systems* in [GK13], where a more general definition of Casimir functions is provided.

Conjecture 8.3. *The constant C in Proposition 8.1 equals 1 for all $k \geq 2$.*

We prove Conjecture 8.3 for $k = 2$ and $k = 3$. Let $x_j = x_j(P)$ be the corner invariants of $[P]$. The case $k = 2$ follows from $y_i^{(2)}(P) = -x_{2i+1}x_{2i+2}$ (see Equation (32)), so

$$\prod_{i=1}^n y_i^{(2)}(P) = (-1)^n \prod_{i=1}^n x_{2i+1}x_{2i+2} = (-1)^n\, O_n(P)\, E_n(P),$$

which is T_2-invariant by Lemma 7.3.

For the case $k = 3$, Equation (31) implies

$$\prod_{i=1}^n y_i^{(3)}(P) = (-1)^n \prod_{i=1}^n \frac{x_{2i}x_{2i+3}}{(x_{2i}-1)(x_{2i+3}-1)} = (-1)^n\, \mathcal{F}_1(P)\, \mathcal{F}_2(P),$$

which is T_3-invariant by Proposition 6.1.

References

[FK12] P. Di Francesco and R. Kedem. T-systems with boundaries from network solutions, 2012. 125

[FM16] V. V. Fock and A. Marshakov. *Loop groups, clusters, dimers and integrable systems*, pages 1–65. Springer International Publishing, Cham, 2016. 125

[FMB19] R. Felipe and G. Marí Beffa. The pentagram map on Grassmannians. *Annales de l'Institut Fourier*, 69(1):421–456, 2019. 125

[GK13] A. B. Goncharov and R. Kenyon. Dimers and cluster integrable systems. *Annales scientifiques de l'École Normale Supérieure*, Ser. 4, 46(5):747–813, 2013. 177

[Gli11] M. Glick. The pentagram map and y-patterns. *Advances in Mathematics*, 227(2):1019–1045, 2011. 124, 125, 168

[Gli18] M. Glick. The limit point of the pentagram map. *International Mathematics Research Notices*, 2020(9):2818–2831, 2018. 125

[GP16] M. Glick and P. Pylyavskyy. Y-meshes and generalized pentagram maps. *Proceedings of the London Mathematical Society*, 112(4):753–797, 2016. 125, 127, 130, 132, 164, 166, 167, 168, 176, 177

[GSTV12] M. Gekhtman, M. Shapiro, S. Tabachnikov, and A. Vainshtein. Higher pentagram maps, weighted directed networks, and cluster dynamics. *Electronic Research Announcements*, 19(0):1–17, 2012. 124, 125, 132, 176, 177

[IK23] A. Izosimov and B. Khesin. Long-diagonal pentagram maps. *Bulletin of the London Mathematical Society*, 55(3):1314–1329, 2023. 125

[Izo22a] A. Izosimov. The pentagram map, poncelet polygons, and commuting difference operators. *Compositio Mathematica*, 158(5):1084–1124, 2022. 125

[Izo22b] A. Izosimov. Pentagram maps and refactorization in poisson-lie groups. *Advances in Mathematics*, 404:108476, 2022. 125

[KS13] B. Khesin and F. Soloviev. Integrability of higher pentagram maps. *Mathematische Annalen*, 357(3):1005–1047, 2013. 125

[KS16] B. Khesin and F. Soloviev. The geometry of dented pentagram maps. *Journal of the European Mathematical Society*, 018(1):147–179, 2016. 125

[KV15] R. Kedem and P. Vichitkunakorn. T-systems and the pentagram map. *Journal of Geometry and Physics*, 87:233–247, 2015. Finite dimensional integrable systems: on the crossroad of algebra, geometry and physics. 125

[MB13] G. Marí Beffa. On generalizations of the pentagram map: discretizations of agd flows. *Journal of Nonlinear Science*, 23(2):303–334, 2013. 125

[MB14] G. Marí Beffa. On integrable generalizations of the pentagram map. *International Mathematics Research Notices*, 2015(12):3669–3693, 2014. 125

[NS21] D. Nackan and R. Speciel. Continuous limits of generalized pentagram maps. *Journal of Geometry and Physics*, 167:104292, 2021. 125

[OST10] V. Ovsienko, R. E. Schwartz, and S. Tabachnikov. The pentagram map: a discrete integrable system. *Communications in Mathematical Physics*, 299(2):409–446, 2010. 124, 125, 127, 131, 140

[OST13] V. Ovsienko, R. E. Schwartz, and S. Tabachnikov. Liouville-arnold integrability of the pentagram map on closed polygons. *Duke Mathematical Journal*, 162(12):2149 – 2196, 2013. 124

[Sch92] R. E. Schwartz. The pentagram map. *Experimental Mathematics*, 1(1):71 – 81, 1992. 124, 127, 128, 129, 135

[Sch01] R. E. Schwartz. The pentagram map is recurrent. *Experimental Mathematics*, 10:519–528, 2001. 124, 130

[Sch07] R. E. Schwartz. The poncelet grid. *Advances in Geometry*, 7(2):157–175, 2007. 125

[Sch08] R. E. Schwartz. Discrete monodromy, pentagrams, and the method of condensation. *Journal of Fixed Point Theory and Applications*, 3(2):379–409, 2008. 124, 125, 127, 131, 137, 138, 159, 174

[Sch13] R. E. Schwartz. Pentagram spirals. *Experimental Mathematics*, 22(4):384–405, 2013. 131

[Sch21] R. E. Schwartz. A textbook case of pentagram rigidity, 2021. 125

[Sch24] R. E. Schwartz. Pentagram rigidity for centrally symmetric octagons. *International Mathematics Research Notices*, 2024(12):9535–9561, 2024. 125, 132, 170

[Sch25] R. E. Schwartz. The flapping birds in the pentagram zoo. *Arnold Mathematical Journal*, page to appear, 2025. 125, 126, 128

[Sol13] F. Soloviev. Integrability of the pentagram map. *Duke Mathematical Journal*, 162(15):2815–2853, 2013. 124

[Wei23] M. H. Weinreich. The algebraic dynamics of the pentagram map. *Ergodic Theory and Dynamical Systems*, 43(10):3460–3505, 2023. 125

AUTHOR

Zhengyu Zou
Department of Mathematics,
Brown University
Providence, RI, USA
email: Zhengyu_Zou@brown.edu